Peer-reviewed version available at *Cells* **2020**, *9*, 755; doi:10.3390/cells9030755

CDC37 and HSP90 are Essential for Stressome Release and Tumor Progression in Resistant Prostate Cancer

Taka Eguchi [1,2,*], Chiharu Sogawa [1], Kisho Ono [3], Masaki Matsumoto [4], Manh Tien Tran [1], Yuka Okusha [1,5], Benjamin J. Lang [5], Kuniaki Okamoto [1], Stuart K. Calderwood [5,*]

[1] Department of Dental Pharmacology, Graduate School of Medicine, Dentistry and Pharmaceutical Sciences, Okayama University, Okayama 700-8525 Japan.

[2] Advanced Research Center for Oral and Craniofacial Sciences, Graduate School of Medicine, Dentistry and Pharmaceutical Sciences, Okayama University, Okayama 700-8525 Japan.

[3] Department of Oral and Maxillofacial Surgery, Okayama University Hospital, Okayama 700-0914 Japan.

[4] Department of Molecular and Cellular Biology, Medical Institute of Bioregulation, Kyushu University, 3-1-1 Maidashi, Higashi-ku, Fukuoka 812-8582, Japan.

[5] Department of Radiation Oncology, Beth Israel Deaconess Medical Center, Harvard Medical School, Boston MA 02115 USA.

† These authors contributed equally to this work.

*Correspondence:

Takanori Eguchi. 2-5-1, Shikata-cho, Okayama 700-8525 Japan. Phone: +81-86-235-6662. Fax: +81-86-235-6664. E-mail: eguchi@okayama-u.ac.jp ; eguchi.takanori@gmail.com

Stuart K. Calderwood. 330 Brookline Avenue / Dana 717A, Boston, MA 02215. Phone: +1 617 667 4240. Fax: +1 617 667 4245. E-mail: scalderw@bidmc.harvard.edu ; StukCalderwood@gmail.com

Peer-reviewed version available at Cells 2020, 9, 755; doi:10.3390/cells9030755

Abstract

Tumor cells exhibit a resistance-associated secretory phenotype involving extracellular vesicles (EVs) and heat shock proteins (HSPs). This response occurs in response to cell stress and cancer therapeutics. HSPs are stress-responsive molecular chaperones promoting proper protein folding, while also being released from cells with EVs as well as in free form as alarmins. We have here investigated the secretory phenotype of castration-resistant prostate cancer (CRPC) cells using proteome analysis. We have also examined the roles of the key co-chaperone CDC37 in stressome release, epithelial-to-mesenchymal transition (EMT), and tumor progression. A number of HSP family members and their common receptor CD91/LRP1 were enriched at high levels in CRPC cell-derived EVs among over 700 other protein species. The small EVs (30 to 200 nm in size, potentially exosomes) were released even in a non-heated condition from the prostate cancer cells, whereas EMT-coupled release of EVs (200 to 500 nm, likely ectosomes) with associated HSP90α was increased after heat shock stress (HSS). Lactate dehydrogenase, a marker of membrane leakage/damage of cells, was also released upon HSS from the prostate cancer cells. During this stress response, intracellular CDC37 was also transcriptionally inducible by heat shock factor 1, and knockdown of CDC37 decreased EMT-coupled release of EVs. Triple knockdown of CDC37, HSP90α, and HSP90β was required for efficient reduction of the chaperone trio and to reduce tumorigenicity of the CRPC cells in vivo. Taken together, the data indicated that CDC37 and HSP90 are essential for stressome release and for tumorigenesis in resistant cancer.

Keywords: cell stress response; stressome; extracellular vesicle; heat shock protein 90 (HSP90); cell division control 37 (CDC37); prostate cancer; exosome; ectosome

Introduction

Tumor cells are often exposed to various stresses such as immune/inflammatory stress, therapeutics [1], hypoxia, acidification, oxidative stress [2,3], starvation [4], nutrient stress [5], heat and cold [6,7], thermal stress, replication stress [8], endoplasmic reticulum (ER) stress, neurotoxic stress [9], genotoxic (DNA damage) [10] and proteotoxic stress [11,12]. Heat shock proteins (HSPs) were originally found to be induced upon heat shock stress (HSS) {Murshid, 2013, Stress proteins in aging and life span}. Later studies have revealed that other types of stresses can also induce HSPs, including hypoxia [13] and nutrient starvation [4]. HSPs are molecular chaperones that assist in proper protein folding and re-folding in the cells, playing stress-resistant roles in anti-apoptotic activity [6] against radiation therapy, chemotherapy, and immunotherapy. It has been shown that HSPs are often increased in tumor cells and are involved in the properties of tumor progression such as increased migration, invasion, and metastasis [14,15]. In addition, extracellular HSPs have been shown to be released from cells with vesicles as well as in free form [16-18]. Notably, it has been shown that HSPs and vesicles were co-released upon cell stress and cell damage such as molecular targeted therapeutic stress [19,20], anti-cancer therapeutic DNA damage stress [21,22], and HSS [23,24]. Extracellular HSPs have been also known as alarmin or damage- / danger-associated molecular patterns (DAMP) that are released from cells upon tissue damage [25,26].

Extracellular vesicles (EVs) are particles surrounded by lipid membranes, containing a variety of molecular cargos such as proteins, small and large RNAs, DNA, lipid, glycans, minerals, and metabolites that are secreted by cells [27-30]. Earlier studies classified the range of EVs into exosomes (50-200 nm), ectosomes (100-500 nm; also known as microvesicles) [31,32], and apoptotic bodies (1-10 μm) based on their mechanisms of generation and release, while additional types of EVs have been reported consisting of oncosomes (named after oncogenic EVs) [33,34], large oncosomes (1-10 μm) [35,36], matrix vesicles [37], migrasomes [38], exopheres (~4 μm), exomeres (~35 nm), and bacterial outer membrane vesicles (OMV) [39]. EVs are also classified by their sizes into small EVs (sEV: 30-500 nm) and large EVs (L-EV: > 1 μm) [35,40]. These vesicles play basic roles in discarding molecules unfavorable for cells [41], while also mediating intercellular communication by transferring their cargos to recipient cells or organs in local and/or distant tissues [42]. Among various concepts of EVs, oncosomes have been shown to promote processes in tumor progression such as epithelial-to-mesenchymal transition (EMT) by transferring oncogenic molecules [43-45]. In addition, the findings that enhancement of EMT properties was coupled with increased release of EVs [20,46] prompted us to make a concept of EMT-coupled vesicle release. Among a number of molecular cargos, HSPs are major signatures often found within sEV such as exosomes, ectosomes, and oncosomes [16-18,25]. Indeed, sEV derived from oral cancer cells contained a

variety of HSPs, including HSP90α, HSP90β, TRAP1 (mitochondrial HSP90), HSP105, HSP70 (HSP72/HSPA1A and HSP70B'/HSPA6), GRP78/HSPA5 (ER chaperone), and heat shock cognate 70 (HSC70: essential for autophagy) [17]. Notably, two HSP90 isoforms- HSP90α and HSP90β were enriched in sEV derived from high metastatic cancer cells compared to low metastatic ones [17]. The high expression levels of HSP90α/β are correlated with poor prognosis in patients suffering from head and neck cancers [17]. A number of studies, including ours, have indicated that HSP90 is essential in stress resistance in cancer cells [16,47-49]. Notably, HSP90α and its key co-chaperone CDC37 were highly expressed in resistant prostate cancer cells [18,50]. However, less is known regarding stress-responsive co-release of EVs and HSP90 from the resistant cells. We have therefore addressed this deficiency in this study.

The growth of prostate cancers is often androgen-dependent, requiring factors such as testosterone and dihydrotestosterone (DHT) [51]. Therefore, androgen depletion therapy (ADT), also called hormone therapy is often effective in prostate cancers. However, some types of prostate cancer are resistant to ADT. These castration-resistant prostate cancers (CRPC) are known as neuroendocrine tumors (NET), and this is also a phenotype found in aggressive pancreatic cancer [52-54]. Notably, tumorigenicity and epithelial-to-mesenchymal transition (EMT) are key properties for recurrence and metastasis in such aggressive, resistant cancers [55,56]. In the androgen insensitivity, intracellular kinase signaling pathways are given higher priorities required for tumor progression. Indeed, it has been shown that CDC37, the protein kinase-specialized (kinome) co-chaperone of HSP90, were highly expressed in the resistant prostate cancer cells [57]. CDC37 plays a fundamental role in chaperoning almost all members of the protein kinase family and participates in cancer by maintaining the activity of protein kinases involved in cell proliferation and transformation [58,59]. These include tyrosine kinases such as Src [60], and serine/threonine kinases in the Raf-ERK pathway [61], Akt, the inhibitor of NF-κB kinase (IKK) [62], and cyclin-dependent kinase 4 (CDK4) [63,64]. CDC37 functions primarily in a complex with HSP90 to mediate the 3-dimensional (3D) folding and structural integrity of client proteins kinases [60,65]. CDC37 is particularly significant in prostate cancer as its overexpression leads to spontaneous prostate carcinogenesis in transgenic mice [66]. It has also been suggested that the high levels of oncogenic proteins present in most cancers make them dependent on molecular chaperones, a state referred to as "chaperone addiction" [58]. Thus, because of their large protein clienteles, the CDC37-HSP90 axis offers a critical target for inactivating multiple oncogenic pathways. Consequently, the inhibition of HSP90 in cancer is currently a major area of research [67,68]. However, less is known regarding the role of CDC37 in EV release and we have addressed this deficiency in this study.

Peer-reviewed version available at *Cells* **2020**, *9*, 755; doi:10.3390/cells9030755

In the present study, we therefore aimed (i) to reveal proteome signatures of EVs derived from resistant prostate cancer cells, (ii) to unveil stress-responsive vesicle release potentially coupled with resistant tumorigenicity in cancer.

Materials and Methods

Cell culture. PC-3, a CRPC cell line, and DU-145, a prostate adenocarcinoma cell line, were maintained in RPMI1640 medium with 5% to 10% FBS as described previously [18,57,69,70]. RWPE1, a human normal prostate cell line, was maintained in keratinocyte serum-free medium (ThermoFisher, Waltham, MA) supplemented with recombinant human epidermal growth factor and bovine pituitary extract.

Heat shock stress. For HSS, the medium was replaced to incubated medium at 43°C or 37°C and then put in a water bath at 43°C or 37°C, as described previously [23,71]. After HSS, cells were washed with PBS (-) and cultured in serum-free media. Cellular photomicrographs were taken at 24 h after medium replacement by using Floid Cell Imaging Station (ThermoFisher).

Extracellular vesicle and non-EV fractions. For HSS experiments, after the above-mentioned HS, cells were washed with PBS and cultured in serum-free media for 24 h and then conditioned media was collected. At the time of harvest, the numbers of cells were counted using Countess (ThermoFisher) and whole cell lysate was prepared as described below. Otherwise, cultured cells were washed with Hanks' balanced salt solution (HBSS), and then further cultured in serum-free medium for 1 or 2 days. EV fraction was prepared using a modified polymer-based precipitation (PBP) method. Briefly, the conditioned medium was centrifuged at 2,000 × *g* for 30 min at 4°C to remove cell debris. For studies of knockdown and EMT, the supernatant was filtered with a 0.2-μm syringe filter. Otherwise, the filter was not used. The supernatant was collected and centrifuged at 10,000 × *g* for 30 min at 4°C. The supernatant was collected and applied to an Amicon Ultra-15 Centrifugal Filter Device MW.100k (Merck, Kenilworth, NJ) to concentrate the pre-EV fraction to less than 1 ml and to separate non-EV soluble fraction. The pass-through was applied to an Amicon Ultra-4 Centrifugal Filter Device MW.10k (Merck) to concentrate the non-EV soluble fraction. Total Exosome Isolation Reagent (ThermoFisher) was applied to the pre-EV fraction and incubated overnight at 4°C. The precipitated EVs were collected by centrifugation at 10,000 × *g* for 60 min at 4°C. For biological assays, the EV fractions were eluted in 100 μl PBS (−). For protein assay, 10 × RIPA buffer containing 10% NP-40, 1% SDS, 5% deoxycholate in PBS (-), and a protease

Peer-reviewed version available at Cells 2020, 9, 755; doi:10.3390/cells9030755

inhibitor cocktail (Sigma) was added to the EV fraction, incubated on ice for 15 min. The EV-derived protein samples were quantified with a principle of bicinchoninic acid (BCA) method using Micro BCA protein assay system (ThermoFisher). EV protein concentrations per cell were calculated at the time points of harvest.

Mass spectrometry. EV fraction was incubated in the presence of 1% SDS and 2.5 mM Tris (2-carboxyethyl)phosphine hydrochloride (ThermoFisher) for 10 min at 85°C followed by alkylation with 12.5 mM iodoacetamide (Sigma) for 15 min at room temperature. Proteins were precipitated with acetone for 2 h at -30°C and the resulting pellet was dispersed in 100 mM ammonium bicarbonate by ultrasonic treatment (three times for 30 s with intervals of 30 s) with a Bioruptor (Diagenode). The protein suspension was subjected to digestion with trypsin (1 μg; Wako) for 14 h at 37°C. Resulting peptides were analyzed by a QExactive mass spectrometer that was coupled with nano-LC (AdvanceLC, Michrom Inc.) via a nano-electrospray source with a column oven set at 37°C (AMR Inc.). Samples were injected to pre-column (L-column micro: 0.3 mm inner diameter, 5 mm length; CERI, Japan) and separated by in-house made 20 cm column (inner diameter 100 μm, 3 μL-column; CERI, Japan) with a linear gradient (5–30% B for 110 min, 30–90% B for 1 min, and 90% B for 10 min, A: 0.1% formic acid, 2% acetonitrile, B: 0.1% formic acid, 99.9% acetonitrile) at a flow rate of 250 nl/min. The QExactive was operated in data-dependent acquisition mode. Scan ranges were set at m/z 375−1600 for MS spectra and at m/z 200−2000 for MS/MS spectra, respectively. MS spectra were acquired at a resolution of 70,000 at m/z 400 after accumulation to a target value of 1×10^6 with the maximum ion injection times for 60 msec. Up to the top 10, most abundant ions with charge 2+ or 3+ from the survey scan were selected with an isolation window of 1.5 h and fragmented by HCD with normalized collision energies of 25. MS/MS spectra were acquired at a resolution of 17,500 at m/z 400 after accumulation to a target value of 5×10^4 with the maximum ion injection times for 120 msec. The acquired MS/MS spectra were analyzed by Proteome Discoverer 1.4 with the Mascot algorithm (ver. 2.6.0) using an IPI human database (ver. 3.8.7). The search was performed with the following parameters: Trypsin was selected as an enzyme used, allowed a number of missed cleavages was set 3 and carbamidomethylation on Cys were selected as a fixed modification. Oxidized methionine was searched as variable modifications. Precursor mass tolerances were 10 ppm and tolerance of MS/MS ions was 0.02 Da. The second LC-MS/MS with or without HS was carried out as described [17,72].

Electron microscopy. A 400-mesh copper grid coated with formvar/carbon films was hydrophilically treated. The EV suspension (5 to 10 μl) was placed on parafilm, and the grid was floated on the EV liquid

and left for 15 min. The sample was negatively stained with 2% uranyl acetate solution for 2 min. EVs including exosomes on the grid were visualized with 5,000 to 20,000 times magnification with an H-7650 transmission electron microscope (Hitachi, Tokyo, Japan) at Central Research Laboratory, Okayama University Medical School. To determine the size of EVs, TEM images were analyzed using Image J software. The diameters of fifty EVs were measured by taking the length of the widest point of each EV. Objects were limited to those greater than 50 nm.

Particle diameter distribution analysis. Forty microliters of EV fraction within PBS (-) was used. Particle diameters of the EV fractions in a range between 0 and 10,000 nano-diameters were analyzed in Zetasizer nano ZSP (Malvern Panalytical, UK).

Cytotoxic LDH assay. Cytotoxicity was measured using the index of lactate dehydrogenase (LDH) release from the cells and was expressed as a percentage of total cellular LDH activity. LDH activity was measured using an LDH cytotoxicity assay kit according to the manufacturer's instructions (Nacalai Tesque, Kyoto, Japan). Cells were seeded at 5,000 cells/well in 96-well plate and pre-cultured in RPMI1640 medium containing 10% FBS for 1 or 2 days. After the above-mentioned HSS for 0.5, 1.5 or 3 hours, culture media were collected for the first LDH assay. Cells were washed with PBS (-), cultured in serum-free media for 24 hours, and then conditioned media were collected. The collected culture media were transferred to another 96-well plate and incubated with substrate solution at RT for 20 min. The stop solution was added and absorbance (490 nm) was measured.

Cellular morphology. The rates of occurrence of cells with projections and round-shaped cells in cellular photomicrographs were counted by two researchers as blind experiments.

Promoter analysis. The DNA sequence of the human *CDC37* 5' flanking region and gene body (-2000 to +2000) was obtained from the Eukaryotic Promoter Database [73]. Heat shock element (HSE) was predicted using PROMO [74,75].

Plasmid constructs and luciferase assay. The CDC37 promoter-luciferase reporter constructs (500+utr and 200+utr) was described previously [57]. The overexpression constructs of heat shock factor 1 (HSF1) and dominant-negative (DN)-HSF1 were described previously [71]. Plasmid DNA co-transfection and luciferase assay were performed as described previously [57,71,72]. Briefly, cells were cultured in 96-well plates and a plasmid (25 ng reporter, 100 ng effector) was transfected with 0.4 μl FuGENE HD (Roche,

Basel, Switzerland) per well at a cell confluence level of 50-70%. The medium was changed at 16-20 hours after transfection. At 40-48 hours after transfection, 70 µl of the medium was aspirated, then 30 µl of Bright-Glo reagent (Promega, Madison, WI) was added and mixed by pipetting. Cells were incubated for 5 minutes at 37°C. The lysate (40 µl) was transferred to a 96-well white plate for measurement of luminescence.

RNA interference. We designed siRNA sequences targeting mRNA of *CDC37, HSP90AA1* or *HSP90AB1* (Table 1). For targeting each mRNA, a mixture of two types of siRNA duplex was used. The control non-targeting siRNA was purchased from Nippon Gene. Cells were transfected with siRNA using Lipofectamine RNAi MAX (Thermo Fisher). For single or double knockdown, cells were cultured in a 6-cm dish and 27 pmol siRNA was transfected with 8 µl of Lipofectamine RNAi MAX per dish for 24 hours. The medium was replaced to serum-free fresh ones and the EV and whole cell lysate (WCL) were prepared at 48 hours post-transfection.

Table 1 | List of sequences of siRNA.

Name of siRNA	Sequence (5' to 3')
hCDC37.NM7065-433 sense	gcaagaaggagaagagcauTT
hCDC37.NM7065-433 antisense	augcucuucuccuucuugcTT
hCDC37.NM7065-584 sense	gaaacagaucaagcacuuuTT
hCDC37.NM7065-584 antisense	aaagugcuugaucuguuucTT
hHSP90AA1.NM5348-415 sense	gcugcauauuaaccuuauaTT
hHSP90AA1.NM5348-415 antisense	uauaagguuaauaugcagcTT
hHSP90AA1.NM5348-2010 sense	caaacauggagagaaucauTT
hHSP90AA1.NM5348-2010 antisense	augauucucuccauguuugTT
hHSP90AB1-NM_001271971.1-1353 sense	cagaagacaaggagaauuaTT
hHSP90AB1-NM_001271971.1-1353 antisense	uaauucuccuugucuucugTT
hHSP90AB1-NM_001271971.1-1754 sense	gaagagagcaaggcaaaguTT
hHSP90AB1-NM_001271971.1-1754 antisense	acuuugccuugcucucuucTT

For triple knockdown, electroporation-mediated transfection was optimized and performed as described previously [57,76]. To optimize electroporation for each cell type, cells (1×10^5 to 1×10^6 cells), siRNA (40 pmol total), and serum-free medium were mixed to 100 µl total in a green cuvette with a 1-mm

Preprints (www.preprints.org) | NOT PEER-REVIEWED | Posted: 11 February 2020 doi:10.20944/preprints202002.0148.v1

Peer-reviewed version available at Cells 2020, 9, 755; doi:10.3390/cells9030755

gap (NepaGene, Ichikawa, Tokyo) and set to NEPA21 Super Electroporator (NepaGene). Poring pulse was optimized between 100V and 300V for 2.5 or 5.0 msec pulse length twice with 50 msec interval between the pulses and 10% decay rate with + polarity, as shown in a supplemental figure. The transfer pulse condition was five pulses at 20V for 50 msec pulse length with 50 msec interval between the pulses and 40% decay rate with +/- polarity. After electroporation, cells were recovered in serum-contained media. PC-3 (5×10^5 cells) was transfected with 40 pmol siRNA with poring pulse at 175V for 2.5 msec pulse length twice and then cultured for 4 days for western blotting. Alternatively, transfected PC-3 was cultured for 5 days and 1×10^6 cells were subcutaneously injected to each SCID mouse as described below.

Whole Cell Lysate. Cells were lysed as described previously [17,57,76,77]. Briefly, cells were cultured until being sub-confluent and then washed with PBS (-), treated with 150 to 200 µl/dish of a 1x RIPA buffer containing 1% NP-40, 0.1% SDS, and 0.5% deoxycholate, and a protease inhibitor cocktail (Sigma) in PBS (-), and collected by using a cell scraper. Cells were further lysed by a 25G needle-syringe for 10 strokes and then incubated for 30 min on ice. For protein extraction from RWPE1 cells, cell lysis buffer (150 mM NaCl, 1% NP-40, 1% Na-deoxycholate, 0.1% SDS, 50 mM Tris, pH 7.5, 1 mM PMSF, 25 mM NaF, 2% Triton X-100) containing protease inhibitor cocktail was used. The lysate was centrifuged at 12,000 × *g* for 20 min at 4 °C and the supernatant was used as a WCL. The WCL was diluted 10-fold and protein concentration was measured by using the Micro BCA protein assay system (ThermoFisher).

Western Blotting. In the HSS studies, protein samples corresponding to the same cell numbers were applied to each lane. The protein amount and cell numbers used in each experiment were described in supplementary figures. Briefly, the protein amount equivalent to 1×10^5, 5×10^5, 1×10^6, or 3×10^6 was loaded for analysis of EV fractions. The protein amount equivalent to 2×10^4 or 6×10^4 cells was loaded for analysis of WCL. The protein amount equivalent to 3×10^5 cells was used for protein analysis in the non-EV cell culture supernatant. Protein samples were reduced with β-mercaptoethanol except for CD9 western blotting. The samples were separated by SDS-PAGE in 4-20% TGX-GEL (BioRad) or 10% polyacrylamide gel and transferred to PVDF membrane using a semi-dry method. Anti-CDC37 [1:1000; Cell Signaling Technology (CST), Danvers, MA], anti-HSP90α (1:1000; GeneTex, Irvine, CA), anti-HSP90β (1:1000; GeneTex), anti-CD9 (1:10000 or 1:1000; MBL, Nagoya, Japan), anti-actin (1:200; Sigma), and HRP-conjugated anti-GAPDH (1:5000; FujiFilm Wako) antibodies were used. The blots were visualized with ECL Plus western blotting substrate (Pierce) or Immobilon Forte western HRP substrate (Millipore).

For studies of knockdown, EV addition, and EMT, equal amounts of protein samples in each Western blotting analysis (each 3 µg of protein samples for analysis of EV-CD9 and EV-GAPDH, and each 15 µg of

protein samples for analysis of cellular proteins). For double knockdown studies, each 10 μg of protein samples for analysis of HSP90α, HSP90β, CDC37, E-cadherin, vimentin, and GAPDH was loaded. Protein samples were reduced with β-mercaptoethanol except for CD9 western blotting, separated by SDS-PAGE in 4-20% TGX-GEL (BioRad) or 10% polyacrylamide gel, and transferred to PVDF membrane using a semi-dry method. For EV addition studies, each 10 μg of protein samples for analysis of E-cadherin, N-cadherin, and GAPDH was loaded. Protein samples were reduced with β-mercaptoethanol, separated by SDS-PAGE in 8% polyacrylamide gel, and transferred to PVDF membrane using a wet method. In addition to the above-mentioned antibodies, anti-E-cadherin (1:1000, CST), N-cadherin (1:1000, CST) and anti-Vimentin (1:1000, CST) antibodies were used. The blots were visualized with ECL Plus western blotting substrate (Pierce) or Immobilon Forte western HRP substrate (Millipore).

The images were quantified with the internal control of the actin or GAPDH protein levels and relative quantitative analysis was carried out based on the image band density ratio using ImageJ software (NIH, Bethesda, MD). The quantitative values were shown in supplemental figures.

Tumorigenesis. All animals were held under specific pathogen-free conditions. For chaperone triple-depletion, PC-3 cells (5×10^5) were transfected with siRNA targeting CDC37, HSP90α and HSP90β (17 pmol each) via electroporation and cultured for 5 days. PC-3 transfected with siRNA (1×10^6 cells) was subcutaneously injected to each back of male SCID mice at 6 to 7-weeks old. The major axis (a) and minor axis (b) of tumors were measured with a caliper at day 78 post-injection period. The tumors were deemed to be ellipsoid and the volumes were calculated with a formula as follows: a tumor volume (V) $\fallingdotseq 4\pi ab^2/3$. These studies were carried out in strict accordance with the recommendations in the Guide for the Care and Use of Laboratory Animals of the Japanese Pharmacological Society. The protocol was approved by the Committee on the Ethics of Animal Experiments of the Okayama University (Permit Number: OKU-2016219).

Statistics. Data were expressed as the means ± SD unless otherwise specified. Statistical significance was calculated using GraphPad Prism (GraphPad, La Jolla, CA). Comparisons of 2 were done with an unpaired Student's *t*-test. Three or more mean values were compared using ANOVA Tukey's multiple comparisons test.

Results

The proteome of sEV released by PC-3 cells

To establish a protein signature of sEV released by the CRPC cells, we performed proteomic analysis of extracellular medium using LC-MS/MS. More than 700 protein species were thus identified, including molecular chaperones (total score: 795.5) such as HSP90α and Hsp90β, extracellular signaling proteins (total score: 10759.0) such as thrombospondin 1, extracellular matrix (ECM) proteins (total score: 3964.7) such as fibronectin, agrin, and tenascin, cytoskeletal proteins (total score: 2070.1) such as actin, myosin, and keratin, ECM metabolic enzymes (total score: 1367.8), lipid and cholesterol metabolic proteins (1574.6), coagulation factors, proteinases, proteinase inhibitors, transmembrane proteins such as CD91/LRP1, metabolic and redox regulators, vesicle- and membrane-associated proteins such as annexin A2 and clathrin HC (Fig. 1A, Table 2).

We next examined whether HSP90α could be altered in cells and EVs or released in free form upon proteotoxic damage exerted by HSS at 43°C. HSP90α was abundantly released with EVs as well as non-EV extracellular HSP90 upon HSS for 1.5 or 3 hours (plus 24 hours recovery), while intracellular HSP90α was also increased (Fig. 1B). As a control, we examined CD9 in the HSS study. Vesicular CD9 was increased upon the HSS, while intracellular levels decreased in the CRPC cells, suggesting that cellular CD9 was transmitted to EVs upon HSS.

These findings indicate that HSP90α was released with EVs in response to proteotoxic stress, while non-vesicular HSP90α was also released in response to the HSS.

Preprints (www.preprints.org) | NOT PEER-REVIEWED | Posted: 11 February 2020 doi:10.20944/preprints202002.0148.v1

Peer-reviewed version available at Cells 2020, 9, 755; doi:10.3390/cells9030755

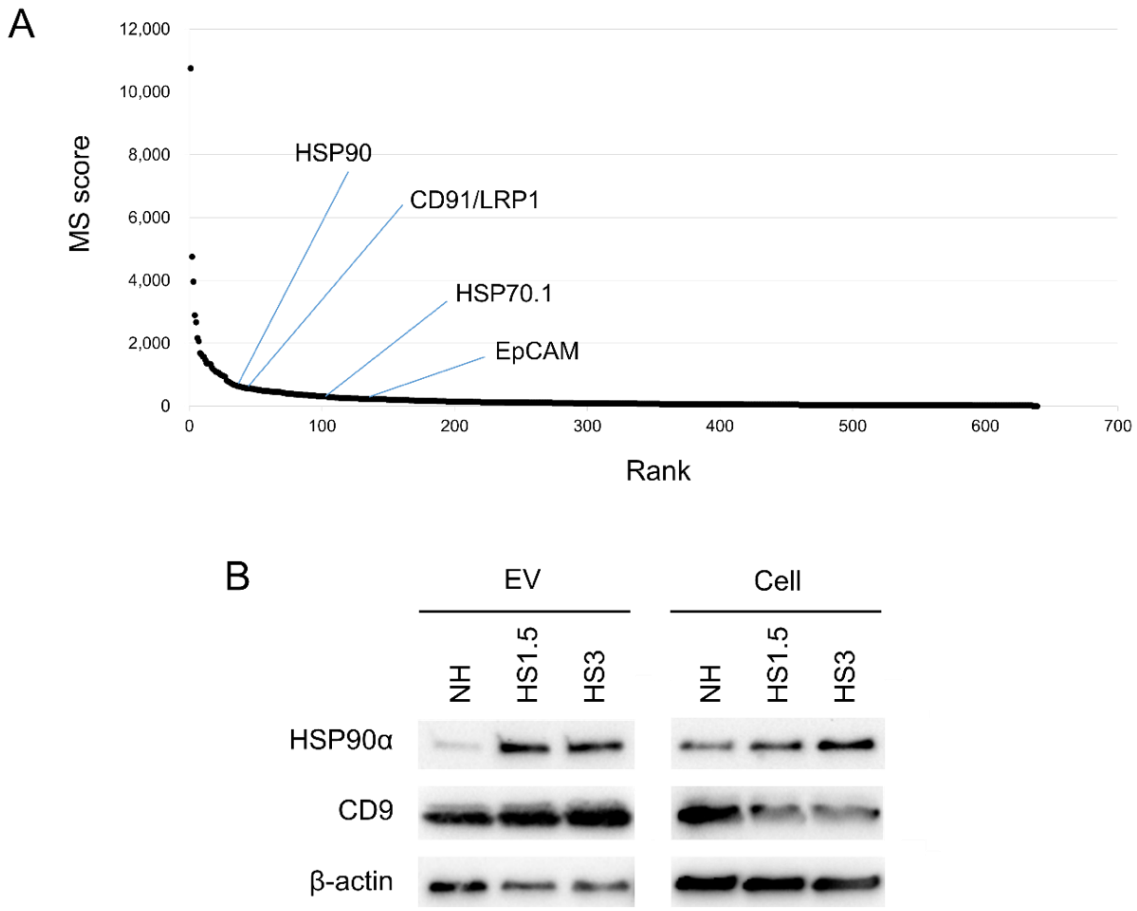

Figure 1 | Proteome and stress response of EVs released by PC-3 cells. (**A**) Scores of proteins identified by LC-MS/MS. (**B**) Western blot showing HSP90α, CD9, and β-actin in EVs and cells. PC-3 cells were stimulated with heat shock stress (HSS) for 1.5 or 3 hours or non-heated (NH) and then cultured in serum-free media to collect EVs and cell lysates.

Table 2. The proteome of EVs released from PC-3 cells.

Class	Summed Scores	Top hit proteins	# of protein species
Extracellular signaling	10759.0	TSP1, LGALS3BP	37
ECM proteins	3964.7	Fibronectin, Agrin, Tenacin	53
Cytoskeletal	2070.1	Actin, Myosin, Keratin	40
ECM metabolic enzymes	1367.8	PLOD1, PXDN	6
Lipid and choresterol metabolism	1574.6	ApoB, ApoA-I	9
Coagulation	1173.8	F2	4
Chaperones, HSP	795.5	HSP90-alpha, Hsp90-beta, HSP70.1	23
Proteinases, proteinase inhibitor	721.6	tPA	17
Transmembrane	582.5	CD91/LRP1, Neuropilin 1	53
Metabolism and Redox	532.7	PKM	51
Vesicle- and membrane-associated	499.6	Annexin A2, Clathrin HC	16
Translational regulators	483.8	EF2	9
Isomerases	285.4	PPIA	7
Hormones	317.4	Inhibin beta	3
Lysosome	364.5	MAN2B1	2
Histone, transcriptional, epigenetic	237.2	H4, H1.4	11
Proteasome	221.0	PSMA7	19
Molecular Traffic	218.6	KIF23	6
G proteins	172.2	RACGAP1, Rac1	13
Calcium signaling	142.8	NBD1	6
Intracellular signaling	135.8	Catenin D1	4
Kinases	133.6	PGK1	7
Phosphatase	94.5	PP2A	6
Ribosome	86.1	Ribosomal protein S28	13
Antimicrobial peptide	47.8	Dermcidin	1
Miscellaneous	340.7	PSAPL1	54
Putatively serum-derived	2673.7	C3	14
Uncharacterized proteins	1544.6	u.c.p.	155

Stress triggered vesicle release (200-500 nm) and cell morphological changes.

We next determined whether the size and morphology of EVs released by the CRPC cells could be altered by HSS. Indeed, the size of EVs released from PC-3 cells without HSS was between 50 nm and 200 nm, while larger EVs sized between 200 nm and 500 nm increased in the medium upon HSS for 30 min, 1.5 hours, and 3 hours (Fig. 2 A, B, C, D). The morphologies of the EVs corresponded basically to a cup-like shape, although the detailed shapes were various (Fig. 2A). The prototypical EVs found under TEM were in a cup-like shape with clear walls potentially composed of a lipid bilayer, although the thickness of the EV walls varied (Fig. 2A a). The wall of an EV was partially thick, which may be associated with another particle (Fig. 2A b). Membrane deformation was also seen in some EVs (Fig. 2A c). Crescent shapes are reminiscent of membrane breakage of EVs (Fig. 2A d). These data suggested that the EVs of 50-200 nm were released from PC-3 cells without HSS, whereas the cells additionally released the larger EVs of 200-500 nm upon stress, the stressome.

Along with the release of the stressome, the morphology of PC-3 cells was altered after HSS (Fig. 2E). The rates of round-shaped cells and cells with projections (or spindle shape) were significantly increased after HSS (Fig. 2 E, F, G). These data suggested that cells could lose intercellular adhesion and junction under stress.

These data suggested that stressome release was coupled with cell morphological changes.

EVs (200-500 nm) were co-released with LDH upon membrane damaging stress

Membrane deformation and break of EVs were potentially induced by the HSS. The membrane deformation of EVs, as well as cells, could trigger the release of HSP90 from the cells and EVs. In order to establish the stress-responsive release of EVs, we next measured the protein concentration of EVs altered by the stress. EV release was significantly increased upon HSS in terms of protein concentration (Fig. 3A). We next hypothesized that cell stress could damage cellular membrane permitting intracellular molecules such as HSPs and lactate dehydrogenase (LDH) to leak, while EVs such as ectosomes could be released by a physiological mechanism. To verify this, we next measured extracellular LDH released from the CRPC cells upon HSS. The release of LDH was increased by HSS for 3 hours as compared to non-heated cells (Fig. 3 B-D). Heat shock, as well as serum starvation stress for 24 hours, increased the release of LDH (Fig. 3 C, D).

These results indicated that HSS induced the release of LDH from the CRPC cells potentially through membrane damage of the cells. sEV and HSP90 could be co-released with LDH upon the membrane damage caused by HSS.

Preprints (www.preprints.org) | NOT PEER-REVIEWED | Posted: 11 February 2020 doi:10.20944/preprints202002.0148.v1

Peer-reviewed version available at Cells 2020, 9, 755; doi:10.3390/cells9030755

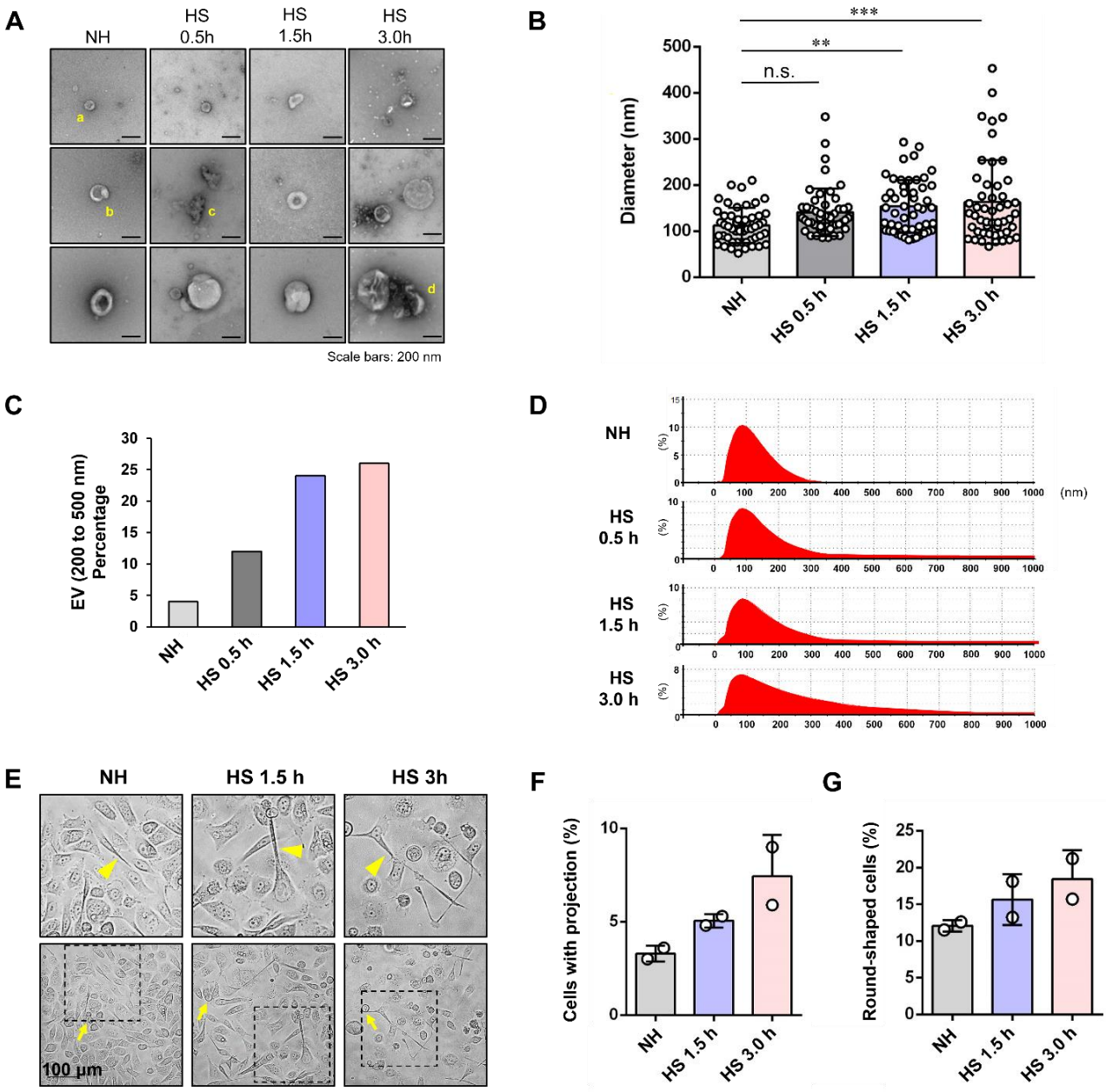

Figure 2 | Release of EVs and membrane damage upon HSS. PC-3 cells were stimulated with HSS for 0.5, 1.5 or 3 hours or NH, cultured for 24 hours in serum-free media, from which EVs were then collected, and images were taken. (**A**) TEM images. **a**, cup-like EVs with clear walls of a potential lipid bilayer. **b**, the wall of an EV was partially thick, which may be associated with another particle. **c**, membrane deformation was also seen in some EVs. **d**, crescent shapes are reminiscent of membrane brake of EVs. Scale bar, 100 nm. (**B**) Column scatterplot analysis of particle size. n=50, mean±SD. ANOVA and Tukey's multiple comparison test was performed for statistics. **P<0.01, ***P<0.001 (vs NH). (**C**) Release of EVs (200-500 nm) upon HSS. (**D**) Particle diameter distribution. Zetasizer was used. (**E-G**) Cell morphological changes upon stress. (**E**) Representative images of cells. Top images were enlarged ones from the squares in the bottom images. Arrows, round-shaped cells. Arrowheads, cells with projections (or spindle shape). Scale, 100 μm. (**F**) Rate of cells with projections. (**G**) Rate of round-shaped cells.

Preprints (www.preprints.org) | NOT PEER-REVIEWED | Posted: 11 February 2020 doi:10.20944/preprints202002.0148.v1

Peer-reviewed version available at Cells 2020, 9, 755; doi:10.3390/cells9030755

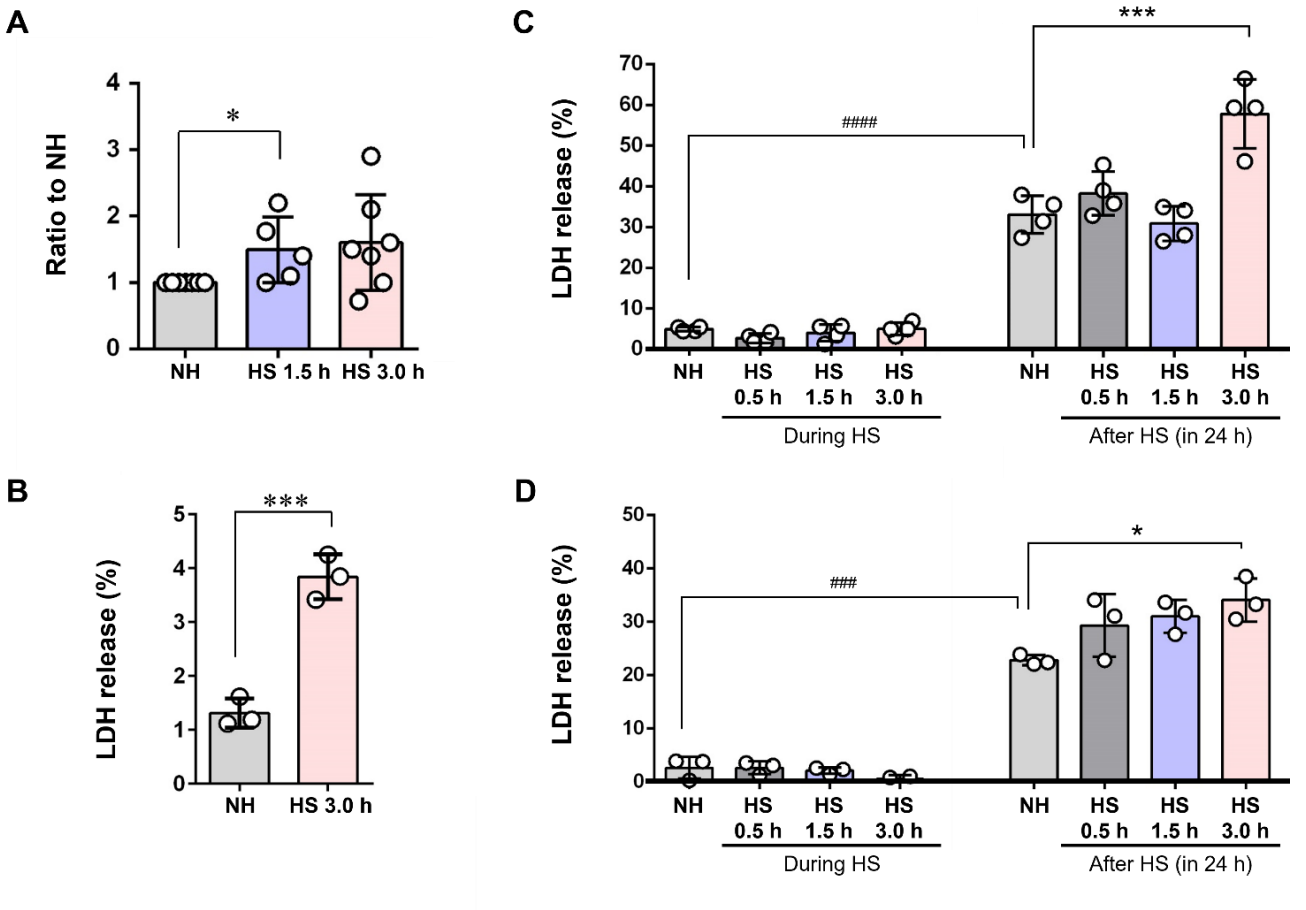

Figure 3 | Release of EVs and membrane damage upon HSS. PC-3 cells were stimulated with HSS for 0.5, 1.5 or 3 hours or NH, cultured for 24 hours in serum-free media, from which EVs were then collected. (**A**) Release of EVs in response to stress. Protein concentrations of EV fractions were quantified using protein assay. *P<0.05, n= 5 to 7. (**B**) Release of LDH upon HSS. PC-3 cells in the sparse condition were stimulated with or without HSS for 3 hours and then LDH release was measured. (**C, D**) Column scatterplot analysis of LDH release. PC-3 cells were stimulated with HSS for 0.5, 1.5 or 3 hours or NH, cultured for 24 hours in serum-free media. The released LDH was measured. Data from two independent experiments were shown in C and D. Statistic analysis was carried out using ANOVA and Tukey's multiple comparisons test. n=3, ***P<0.001, *P<0.05, ###P<0.001, ####P<0.0001

CDC37, a stress-responsive protein essential for the release of EVs.

CDC37 is a molecular chaperone that regulates the folding of kinases and nuclear receptors in association with HSP90. We therefore examined the potential role of this co-chaperone in the release of EVs. Many members of HSP family are stress-responsive, i.e. characteristically inducible by heat shock,

but also by hypoxia, and starvation stress. However, it has not been fully established whether CDC37 could be stress-inducible or not. We next examined whether CDC37 could be transcriptionally inducible by HSS and involved in the release of EVs. We found a heat shock element (HSE) in the promoter region of human *CDC37* gene (Fig. 4 A, B). The consensus HSE sequence is 5'-GAAxxTCCxxGAA-3' while the HSE in the -380 position in the human CDC37 promoter is 5'-GAAagTCCgaGgA-3'. To examine whether the CDC37 promoter could be regulated by heat shock factor 1 (HSF1), we performed the reporter assay using the CDC37 promoter-luciferase constructs. We here used DU-145 prostate adenocarcinoma cells, in which endogenous CDC37 level was not fully induced as compared to the PC-3 cells. The CDC37 promoter (500+utr) containing an HSE (-380) was activated by HSF1 overexpression in DU-145 cells, whereas dominant-negative HSF1 (DN-HSF1) failed to activate the CDC37 promoter (Fig. 4 C, D). Moreover, another CDC37 promoter construct (200+utr) without HSE did not respond to HSF1 overexpression. These data indicated that HSF1 could mediate cell stress signal to the CDC37 gene.

We next examined whether CDC37, HSP90, and CD9 are inducible by HSS in PC-3 cells. As expected, CDC37 was induced by HSS (43°C, 30 min), but not found in either the extracellular or non-vesicular fractions (Fig. 4E, top). HSP90α, a known inducible type of HSP, was increased by HSS intracellularly, in EVs, and in the non-vesicular extracellular fraction (Fig. 4E, second raw). HSP90β, the constitutively expressed HSP90 ortholog was increased in the EV fraction upon the HSS, while intracellular HSP90β was decreased, suggesting that HSP90β could be transmitted from the cells to EV fraction upon the HSS (Fig. 4E, third raw). CD9 was increased in the cells and in the EV fraction upon the HSS (Fig. 4E, fourth raw). These data indicated that CD9-positive exosomes could be secreted from cells upon HSS coordinately with increased CDC37.

These data prompted us to hypothesize that CDC37, although not secreted itself, could be involved in the secretion of CD9-positive exosomes. To verify this hypothesis, we next asked whether the CD9 levels in the EV fraction could be altered by CDC37 knockdown using siRNA. CDC37 knockdown markedly decreased the CD9 level in the EV fraction (Fig. 4F). Coordinately, EV protein concentration per cell was significantly decreased by CDC37 knockdown as compared to the control siRNA condition (Fig. 4G). Cellular protein concentration per cell was also significantly decreased by CDC37 knockdown.

These data suggested that CDC37 was essential for CD9-exosome release and for proteostasis in the CRPC cells.

Preprints (www.preprints.org) | NOT PEER-REVIEWED | Posted: 11 February 2020 doi:10.20944/preprints202002.0148.v1

Peer-reviewed version available at Cells 2020, 9, 755; doi:10.3390/cells9030755

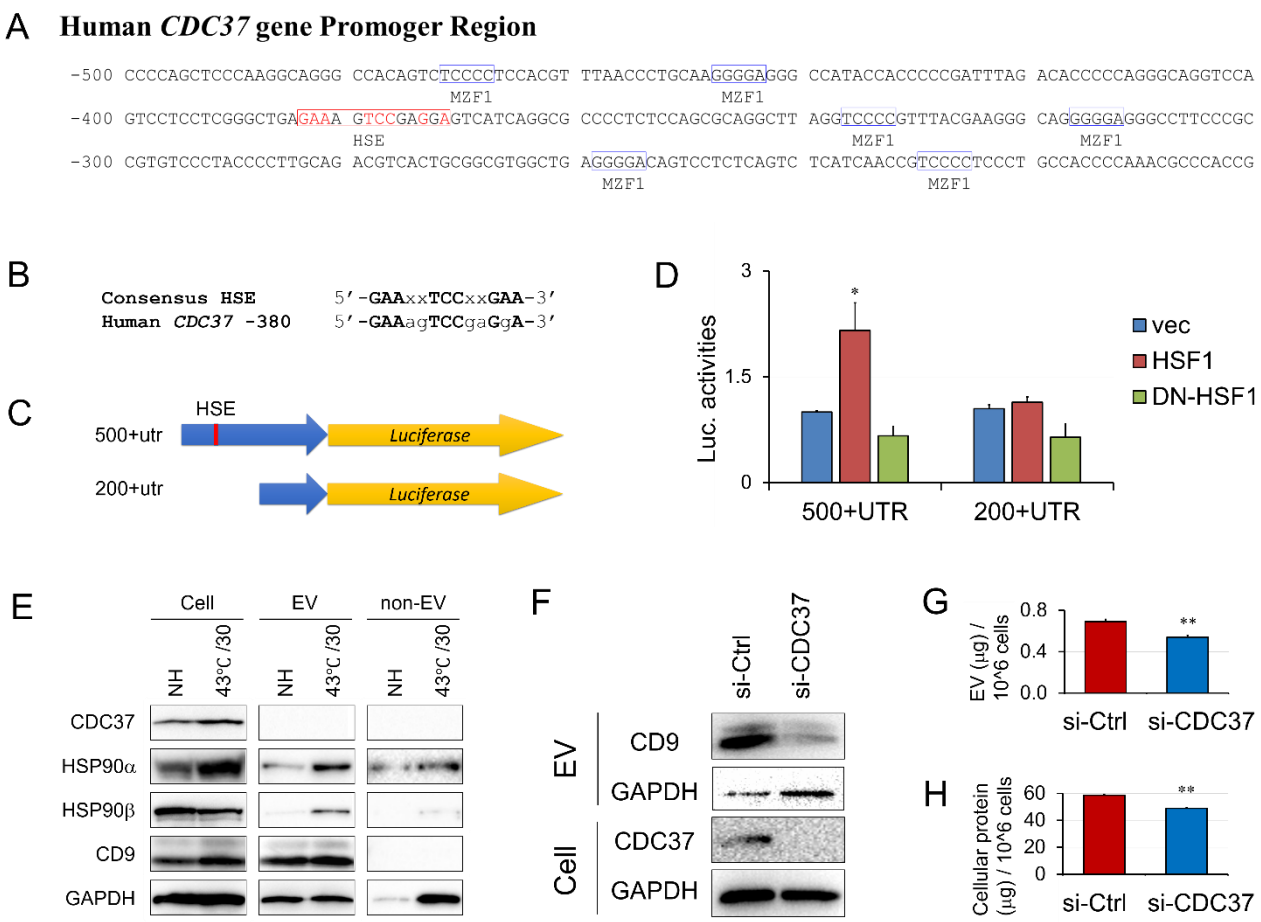

Figure 4 | Expression and roles of CDC37 in vesicle release. (**A**) Analysis of the promoter (-500 to -200) of human CDC37. A heat shock element (HSE) was enclosed with a red rectangle. Red characters are consensus with the typical HSE sequence. MZF1 binding sites were enclosed with blue rectangles. (**B**) Sequences of human CDC37 HSE (-380) and consensus HSE. (**C**) Human CDC37 promoter-luciferase reporter constructs. The 5' flanking regions (500bp + utr or 200bp + utr) were connected with luciferase gene. (**D**) Activities of CDC37 promoter regulated by HSF1. The CDC37 promoter-reporter constructs were co-transfected with overexpression constructs of HSF1 or DN-HSF1 into DU-145 cells. *P<0.05, n=3. (**E**) Western blot showing CDC37, HSP90, CD9, and GAPDH in PC-3 cells, EVs, and non-EV fraction. PC-3 cells were stimulated with or without HSS (43℃ for 30 min) and then cell lysate, EV and non-EV fractions were collected. (**F-H)** Knockdown of CDC37 altered CD9 and protein concentration of EVs. The siRNA targeting CDC37 or non-targeting control siRNA was transfected into PC-3 cells. Cell lysate and EVs were prepared at 48 hours after the transfection from serum-free media. (**F**) Western blot showing CD9 in EV and CDC37 in cells. EVs were prepared using 200-nm pore filter devices and PBP method. (**G**) EV protein concentration per million cells. **P<0.01, n=3. (**H**) Protein concentration per million cells. **P<0.01, n=3.

CDC37 is essential for EMT in the CRPC cells.

The coupling of vesicle release and cell morphological changes upon stress indicated that oncosomes could promote EMT as suggested in Fig. 2. We next aimed to establish whether PC-3-derived EVs could alter EMT properties in the normal prostate epithelial cell line RWPE1. E-cadherin, an established epithelial marker, was decreased by the addition of PC-3-derived EVs in a concentration-dependent manner (0, 5, 10, 25 or 50 μg/ml) (Fig. 5A). In contrast, N-cadherin, an established mesenchymal marker, was increased by the addition of PC-3-derived EVs in a concentration-dependent manner. These data therefore suggested that PC-3-derived EVs could initiate EMT in the prostate epithelial cells.

We next examined whether both CDC37 and HSP90α could be involved in EMT properties in PC-3 cells. We here investigated the vimentin level, a well-established mesenchymal marker. The knockdown of CDC37 markedly decreased vimentin and increased E-cadherin levels in the CRPC cells (Fig. 5B), indicating that CDC37 is an essential factor in EMT. Unlike CDC37, knockdown HSP90α did not decrease vimentin and did increase E-cadherin.

We next examined whether CDC37 and HSP90α could be involved in the release of EVs from PC-3 cells. The knockdown of CDC37 significantly decreased the fraction of EV protein compared with cellular protein concentration, suggesting that EV release was inhibited by CDC37 knockdown (Fig. 5C). In contrast, knockdown of HSP90α did not decrease EV release.

These data indicated that CDC37 was essential for CD9-exosome release and for EMT in prostate cancer cells.

Triple targeting of CDC37, HSP90α, and HSP90β declines the tumorigenicity of CRPC in vivo.

We have experienced that knockdown of a chaperone could often trigger the compensatory induction of another chaperone. We therefore next examined double knockdown and triple knockdown of the chaperone trio- CDC37, HSP90α, and HSP90β. Each combination of siRNA successfully reduced their respective targets, while triple siRNA combination markedly reduced the CDC37, HSP90α, and HSP90β trio (Fig. 5D). Previous studies have shown that PC-3, a CRPC cell line, was the most tumorigenic prostate cancer cell line as compared to the other established prostate carcinoma cell lines. We next examined whether the triple knockdown of the chaperone trio (CDC37, HSP90α, HSP90β) could alter in vivo tumorigenesis of the CRPC cells. The triple knockdown of the chaperone trio markedly inhibited in vivo tumorigenesis of PC-3 cells (Fig. 5E).

Preprints (www.preprints.org) | NOT PEER-REVIEWED | Posted: 11 February 2020 doi:10.20944/preprints202002.0148.v1

Peer-reviewed version available at Cells 2020, 9, 755; doi:10.3390/cells9030755

These results indicated that members of the chaperone trio (CDC37, HSP90α, HSP90β) were complementary to each other and essential for tumorigenicity of the resistant prostate cancer cells.

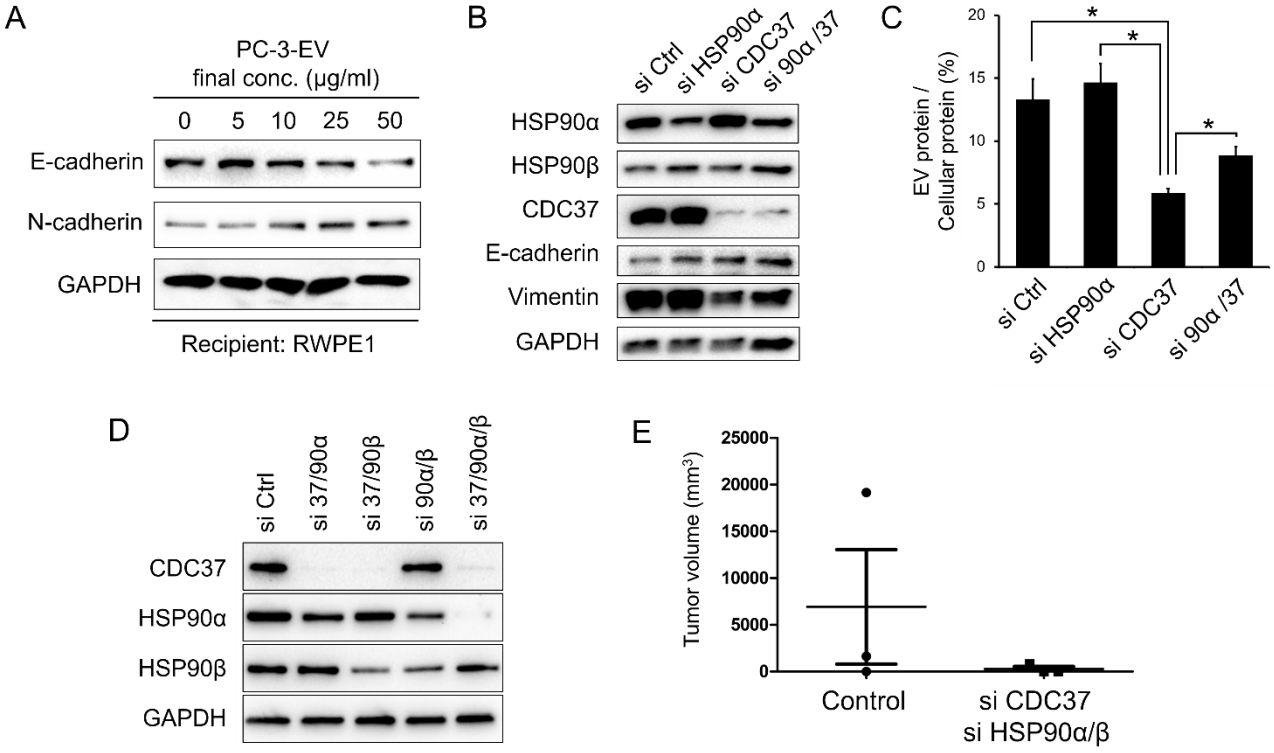

Figure 5 | Vesicle release, EMT and tumorigenicity declined by targeting CDC37 and HSP90. (**A**) Western blot showing E-cadherin/CDH1, N-cadherin/CDH2, and GAPDH. EVs were prepared using 200-nm pore filter devices and PBP method from culture media of PC-3. RWPE-1 cells were treated with the PC-3-derived EV at 0, 5, 10, 25 or 50 μg/ml for 3 days and then lysed. (**B, C**) PC-3 cells were transfected with siRNA targeting CDC37, HSP90α, their combination or non-targeting control siRNA for 48 hours and then cell lysates and EVs were collected. (**B**) Western blot showing CDC37, vimentin, E-cadherin, HSP90, and GAPDH. (**C**) The ratio of EV vs cellular protein concentrations. *P<0.05, n=3. (**D**) Western blot showing CDC37 and HSP90 reduced by double or triple knockdown. siRNA targeting CDC37, HSP90α, and HSP90β or non-targeting control siRNA were transfected into PC-3 cells and then cells were lysed at 48 hours post-transfection. Efficiencies of double or triple knockdown were tested. (**E**) In vivo tumorigenesis declined by triple chaperone knockdown. PC-3 cells were transfected with triple siRNA combination (CDC37, HSP90α, HSP90β) or non-targeting control siRNA and then cells were subcutaneously injected to SCID mice. Data were expressed as Mean±SD, n=3.

Discussion

Cell extrinsic molecules secreted by both tumor and infiltrating normal cells may play key roles in conditioning the tumor environment and enhancing malignancy. For instance, infiltrating macrophages and fibroblasts may supply key growth factors and ECM molecules enhancing growth and metastasis [78-80]. Tumors may also condition their own environments with molecules such as HSPs to supply essential chaperones to recipient cells and trigger receptor-mediated signaling [16,81]. However, the exact details of the tumor chaperone network are not yet defined. Our study demonstrated that HSP90 and CDC37 are essential for a key component of the network, stressome release which permits the exit of HSPs and promotes tumor progression in resistant prostate cancer. The release of EVs and HSP90 from the CRPC cells was a major aspect of the resistance-associated secretory phenotype (RASP). Moreover, we show intracellular CDC37 to be essential for EMT-coupled EV release from CRPC cells, which may constitute a key first step to understanding the mechanisms underlying HSP-loaded EV secretion. There are more than ten co-chaperones of HSP90, which individually carry out distinct cooperative roles with HSP90 in cells [82]. CDC37 is a definitive kinome chaperone assisting in the folding of protein kinases such as SRC, many receptor tyrosine kinases (RTK), their downstream Ras/Raf/MEK/ERK signaling pathway, and PI3K-AKT signaling pathway, which promote EMT [83-86]. Among such key kinases, a recent study showed that SRC in endosomal membranes promoted exosome secretion and tumor progression [87]. Moreover, activation of the epidermal growth factor receptor (EGFR) promoted the secretion of EGFR-rich EVs, whose transmission to recipient cells promoted EMT and metastasis [45,88-91]. LRP1/CD91 is potentially another such an RTK, a receptor whose tyrosine residue in the intracellular domain is phosphorylated by extracellular HSP90 and activates MEK-ERK signaling pathway [92]. CDC37 could positively regulate EMT and exosome release through permitting the function of these protein kinases. Consistently, recent studies have shown that EMT in cancer cells was often coupled with exosome release and drug resistance [20,93,94].

Our studies also touch upon the induced release of HSP90 in the resistant prostate cancer cells. A number of studies, including ours, have indicated that HSP90 is essential in stress resistance in cancer cells [16-18,47,49]. Notably, extracellular HSP90 plays key roles in tumor progression and metastasis as well as immune surveillance [25]. However, mechanisms by which HSP90 is released from cells had not well-investigated before our study. We demonstrated HSP90α to be robustly inducible by HSS and efficiently released as a cargo of EV as well as in the form of EV-free HSP90. In contrast, the HSP90β ortholog was not markedly inducible but was transmitted to EVs upon HSS and barely dissolved in the extracellular fluid. Notably, LDH, GAPDH, HSP90α, and ectosomes/stressome were co-released from cells

Preprints (www.preprints.org) | NOT PEER-REVIEWED | Posted: 11 February 2020 doi:10.20944/preprints202002.0148.v1

Peer-reviewed version available at Cells 2020, 9, 755; doi:10.3390/cells9030755

upon HSS, suggesting that cellular membrane, as well as vesicular membranes, were damaged by the stress. Indeed, extracellular HSPs have been known to exhibit the functions of DAMPs. Moreover, membrane-bound HSPs can be associated with stress-responsive EVs [25]. Along with such released structures, sEV (200-500 nm) were co-released upon HSS, while membrane damage of sEV was also observed upon HSS (Fig. 3). Production of ectosomes (100-500 nm) requires budding and shedding of the cell membrane, which can create membrane damage on cells and vesicles. Moreover, it has been shown that cell motility and stem cell properties induced by the EMT required destabilization of lipid rafts [95]. Therefore, it is conceivable that heat shock triggers the co-release of ectosomes, HSP90, and LDH through membrane damage and destabilization of lipid rafts. A recent study showed that HSP90 mediated membrane deformation and exosome release [96]. However, in our study, knockdown of HSP90 did not decrease the release of vesicles, while, as mentioned above, knockdown of CDC37 significantly decreased the release of EVs, including CD9-exosomes, from the CRPC cells. Therefore, it was conceivable that the chaperone activity of CDC37 was essential for the release of sEV.

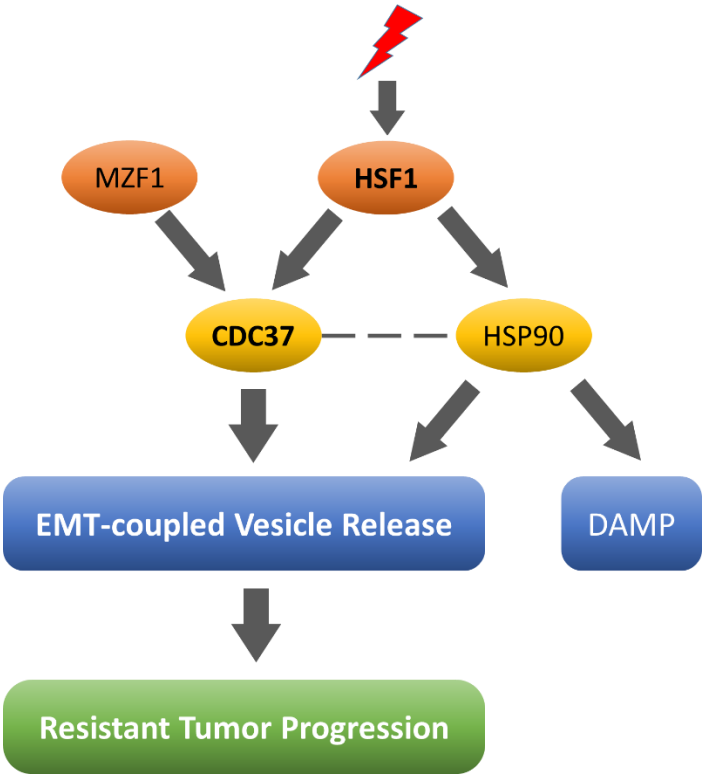

Figure 6 | Graphical abstract. CDC37 and HSP90 are crucial in EMT-coupled vesicle release and resistant tumor progression. High expression of CDC37 in prostate cancer can be enhanced by MZF1 as shown in a recent study [57], while HSF1 can coordinately activate CDC37 gene upon cell stress. Ectosomes and HSP90 (as a DAMP) are co-released upon membrane damage.

It is also clear that the properties of 3D tumors in vivo might be largely different in many aspects from 2D-cultured cells in vitro. Single targeting of CDC37 did not inhibit in vivo tumorigenicity, while triple targeting of CDC37/HSP90α/HSP90β markedly inhibited tumorigenicity of CRPC cells. Consistently, HSP90α was markedly released from 3D tumoroids of PC-3 cells, which resemble a miniaturized tumor in vitro. Thus, the chaperone trio composed of CDC37 and HSP90α/β was crucial for tumorigenicity of CRPC cells. Notably, the tumorigenicity of CRPC cells is a key property for recurrence and metastasis in this type of prostate cancer. In the androgen insensitivity, intracellular kinase signaling pathways can be of higher priority required for tumor progression. This logic is consistent with elevated expression of CDC37, a kinome chaperone, in CRPC as compared to prostate adenocarcinoma and with the anti-tumor effect of the triple chaperone depletion.

Our data also indicated that HSF1, a mediator of the stress response, positively regulates CDC37 gene expression. We recently demonstrated that myeloid zinc finger 1 (MZF1) and SCAND1 reciprocally regulated CDC37 gene expression in prostate cancer. In this study, a gain of MZF1, as well as a loss of SCAND1, were crucial for CDC37 expression. Intracellular matrix metalloproteinase (MMP) 3, a moonlighting transcription factor, also cooperated with HSF1-mediated stress response [71,72,97]. Thus, HSF1 can coordinately activate the CDC37 gene along with other transcription factors, while especially playing a key role in stress response and resistance. Indeed, the overexpression of a DN-HSF1 construct inhibited aneuploidy in prostate carcinoma cells [98]. Thus, HSF1 activation of CDC37 could be crucial for exosome release as well as EMT.

In conclusion, CDC37 and HSP90 are essential for stressome release and EMT-associated tumor progression in resistant prostate cancer. The release of sEV and HSP90 is a major aspect of RASP. Of note, intracellular CDC37 is essential for EMT-coupled EV release from the resistant prostate cancer cells. Future studies are aimed at defining the exact role of CDC37 in the formation and release of tumor EVs.

Author Contributions: TE conceptualized, designed and managed the study, acquired funding, performed heat shock experiments, sampling, promoter analysis, reporter gene assay, animal experiments, and wrote the manuscript. CS performed heat shock experiments, western blotting, TEM, particle diameter analysis, LDH assay, and statistical analysis and wrote the method section. KOn performed particle diameter analysis, cell morphology analysis, siRNA transfection, western blotting, statistical analysis, and wrote the method section and supplementary figure legends. MM performed mass spectrometry. MTT performed western blotting. YO performed cell morphology analysis. BJL performed pilot experiments. KOk supervised TE, CS, KO, and MTT. SKC conceptualized the study, acquired funding, and edited the manuscript. All authors reviewed the manuscript. All authors reviewed the manuscript.

Acknowledgments: The authors thank Eman Ahmed Taha, Yanyin Lu, and Kohei Satoh for illuminating discussion and technical assistance, Akira Sasaki for mentorship and support, Haruo Urata for the operation of TEM, and Kazuko Kobayashi for the operation of Zetasizer.

Funding: This work was funded by JSPS Kakenhi grants: 17K11642 (TE), 17K11643 (CS,TE), 17K11669 (KOh,TE), 18K09789 (KN,TE), 19H04051 (HO,TE), 19H03817 (MT,TE), 19K24072 (KOn), by Suzuken Memorial Foundation (TE), Ryobi Teien Memorial Foundation (CS, KOk, TE), and by NIH under Grant CA176326-05 (SKC).

Conflicts of Interest: The authors declare no conflict of interest.

Abbreviations

CDC37	cell division control 37
CRPC	castration-resistant prostate cancer
DAMP	damage-associated molecular pattern, danger-associated molecular pattern
ECM	extracellular matrix
EGFR	epidermal growth factor receptor
EMT	epithelial-mesenchymal transition
EV	extracellular vesicle
GAPDH	glyceraldehyde-3-phosphate dehydrogenase
HSE	heat shock element
HSF1	heat shock factor 1
HSP	heat shock protein
HSS	heat shock stress
LDH	lactate dehydrogenase
LRP1	low-density lipoprotein-related protein 1
MS	mass spectrometry
NH	non-heated
RASP	resistance-associated secretory phenotype
RTK	receptor tyrosine kinase
sEV	small extracellular vesicle
siRNA	small interfering RNA
TEM	transmission electron microscopy

References

1. D'Orazi, G.; Cirone, M. Mutant p53 and Cellular Stress Pathways: A Criminal Alliance That Promotes Cancer Progression. *Cancers (Basel)* **2019**, *11*, doi:10.3390/cancers11050614.
2. Dias, T.R.; Samanta, L.; Agarwal, A.; Pushparaj, P.N.; Panner Selvam, M.K.; Sharma, R. Proteomic Signatures Reveal Differences in Stress Response, Antioxidant Defense and Proteasomal Activity in Fertile Men with High Seminal ROS Levels. *Int J Mol Sci* **2019**, *20*, doi:10.3390/ijms20010203.
3. Patinen, T.; Adinolfi, S.; Cortés, C.C.; Härkönen, J.; Deen, A.J.; Levonen, A.-L. Regulation of stress signaling pathways by protein lipoxidation. *Redox Biology* **2019**, doi:10.1016/j.redox.2019.101114.
4. Plakidou-Dymock, S.; McGivan, J.D. Amino acid deprivation-induced stress response in the bovine renal epithelial cell line NBL-1: induction of HSP 70 by phenylalanine. *Biochim Biophys Acta* **1994**, *1224*, 189-197, doi:10.1016/0167-4889(94)90190-2.
5. Saito, Y.; Li, L.; Coyaud, E.; Luna, A.; Sander, C.; Raught, B.; Asara, J.M.; Brown, M.; Muthuswamy, S.K. LLGL2 rescues nutrient stress by promoting leucine uptake in ER+ breast cancer. *Nature* **2019**, doi:10.1038/s41586-019-1126-2.
6. Murshid, A.; Eguchi, T.; Calderwood, S.K. Stress proteins in aging and life span. *Int J Hyperthermia* **2013**, *29*, 442-447, doi:10.3109/02656736.2013.798873.
7. Vihervaara, A.; Mahat, D.B.; Guertin, M.J.; Chu, T.; Danko, C.G.; Lis, J.T.; Sistonen, L. Transcriptional response to stress is pre-wired by promoter and enhancer architecture. *Nat Commun* **2017**, *8*, 255, doi:10.1038/s41467-017-00151-0.
8. Xu, B.; Sun, Z.; Liu, Z.; Guo, H.; Liu, Q.; Jiang, H.; Zou, Y.; Gong, Y.; Tischfield, J.A.; Shao, C. Replication stress induces micronuclei comprising of aggregated DNA double-strand breaks. *PLoS One* **2011**, *6*, e18618, doi:10.1371/journal.pone.0018618.
9. Melentijevic, I.; Toth, M.L.; Arnold, M.L.; Guasp, R.J.; Harinath, G.; Nguyen, K.C.; Taub, D.; Parker, J.A.; Neri, C.; Gabel, C.V., et al. C. elegans neurons jettison protein aggregates and mitochondria under neurotoxic stress. *Nature* **2017**, *542*, 367-371, doi:10.1038/nature21362.
10. Gong, J.L.; Lang, B.J.; Weng, D.S.; Eguchi, T.; Murshid, A.; Borges, T.J.; Doshi, S.; Song, B.Z.; Stevenson, M.A.; Calderwood, S.K. Genotoxic stress induces Sca-1-expressing metastatic mammary cancer cells. *Molecular Oncology* **2018**, *12*, 1249-1263, doi:10.1002/1878-0261.12321.
11. Chou, S.D.; Prince, T.; Gong, J.; Calderwood, S.K. mTOR is essential for the proteotoxic stress response, HSF1 activation and heat shock protein synthesis. *PLoS One* **2012**, *7*, e39679, doi:10.1371/journal.pone.0039679.
12. Guang, M.H.Z.; Kavanagh, E.L.; Dunne, L.P.; Dowling, P.; Zhang, L.; Lindsay, S.; Bazou, D.; Goh, C.Y.; Hanley, C.; Bianchi, G., et al. Targeting Proteotoxic Stress in Cancer: A Review of the Role that Protein Quality Control Pathways Play in Oncogenesis. *Cancers (Basel)* **2019**, *11*, doi:10.3390/cancers11010066.
13. Jayaprakash, P.; Dong, H.; Zou, M.; Bhatia, A.; O'Brien, K.; Chen, M.; Woodley, D.T.; Li, W. Hsp90alpha and Hsp90beta together operate a hypoxia and nutrient paucity stress-response mechanism during wound healing. *J Cell Sci* **2015**, *128*, 1475-1480, doi:10.1242/jcs.166363.
14. Ciocca, D.; Clark, G.; Tandon, A.; Fuqua, S.; Welch, W.; McGuire, W. Heat shock protein hsp70 in patients with

axillary lymph node-negative breast cancer: prognostic implications. *J Natl Cancer Inst* **1993**, *85*, 570-574.

15. Eguchi, T.; Lang, B.J.; Murshid, A.; Prince, T.; Gong, J.; Calderwood, S.K. Regulatory roles for Hsp70 in cancer incidence and tumor progression. In *Frontiers in Structural Biology*, Galigniana, M.D., Ed. Bentham Science: 2018; Vol. 1, pp. 1-22.
16. Eguchi, T.; Ono, K.; Kawata, K.; Okamoto, K.; Calderwood, S.K. Regulatory Roles of HSP90-Rich Extracellular Vesicles. In *Heat Shock Protein 90 in Human Diseases and Disorders*, Asea, A.A.A., Kaur, P., Eds. Springer Nature: 2019; pp. 3-17.
17. Ono, K.; Eguchi, T.; Sogawa, C.; Calderwood, S.K.; Futagawa, J.; Kasai, T.; Seno, M.; Okamoto, K.; Sasaki, A.; Kozaki, K.I. HSP-enriched properties of extracellular vesicles involve survival of metastatic oral cancer cells. *J Cell Biochem* **2018**, doi:10.1002/jcb.27039.
18. Eguchi, T.; Sogawa, C.; Okusha, Y.; Uchibe, K.; Iinuma, R.; Ono, K.; Nakano, K.; Murakami, J.; Itoh, M.; Arai, K., et al. Organoids with Cancer Stem Cell-like Properties Secrete Exosomes and HSP90 in a 3D NanoEnvironment. *PLOS ONE* **2018**, *13*, e0191109, doi:10.1371/journal.pone.0191109.
19. Montermini, L.; Meehan, B.; Garnier, D.; Lee, W.J.; Lee, T.H.; Guha, A.; Al-Nedawi, K.; Rak, J. Inhibition of oncogenic epidermal growth factor receptor kinase triggers release of exosome-like extracellular vesicles and impacts their phosphoprotein and DNA content. *J Biol Chem* **2015**, *290*, 24534-24546, doi:10.1074/jbc.M115.679217.
20. Fujiwara, T.; Eguchi, T.; Sogawa, C.; Ono, K.; Murakami, J.; Ibaragi, S.; Asaumi, J.; Okamoto, K.; Calderwood, S.; Kozaki, K. Anti-EGFR antibody cetuximab is secreted by oral squamous cell carcinoma and alters EGF-driven mesenchymal transition. *Biochem Biophys Res Commun.* **2018**, *503*, 1267-1272.
21. Samuel, P.; Mulcahy, L.A.; Furlong, F.; McCarthy, H.O.; Brooks, S.A.; Fabbri, M.; Pink, R.C.; Carter, D.R.F. Cisplatin induces the release of extracellular vesicles from ovarian cancer cells that can induce invasiveness and drug resistance in bystander cells. *Philos Trans R Soc Lond B Biol Sci* **2018**, *373*, doi:10.1098/rstb.2017.0065.
22. Lv, L.H.; Wan, Y.L.; Lin, Y.; Zhang, W.; Yang, M.; Li, G.L.; Lin, H.M.; Shang, C.Z.; Chen, Y.J.; Min, J. Anticancer drugs cause release of exosomes with heat shock proteins from human hepatocellular carcinoma cells that elicit effective natural killer cell antitumor responses in vitro. *J Biol Chem* **2012**, *287*, 15874-15885, doi:10.1074/jbc.M112.340588.
23. Clayton, A.; Turkes, A.; Navabi, H.; Mason, M.D.; Tabi, Z. Induction of heat shock proteins in B-cell exosomes. *J Cell Sci* **2005**, *118*, 3631-3638, doi:10.1242/jcs.02494.
24. Lancaster, G.I.; Febbraio, M.A. Exosome-dependent trafficking of HSP70: a novel secretory pathway for cellular stress proteins. *J Biol Chem* **2005**, *280*, 23349-23355, doi:10.1074/jbc.M502017200.
25. Taha, E.A.; Ono, K.; Eguchi, T. Roles of Extracellular HSPs as Biomarkers in Immune Surveillance and Immune Evasion. *Int J Mol Sci* **2019**, *20*, doi:10.3390/ijms20184588.
26. Harris, H.E.; Raucci, A. Alarmin(g) news about danger: Workshop on Innate Danger Signals and HMGB1. *EMBO Reports* **2006**, *7*, 774-778, doi:10.1038/sj.embor.7400759.
27. Yanez-Mo, M.; Siljander, P.R.; Andreu, Z.; Zavec, A.B.; Borras, F.E.; Buzas, E.I.; Buzas, K.; Casal, E.; Cappello, F.; Carvalho, J., et al. Biological properties of extracellular vesicles and their physiological functions. *J Extracell Vesicles* **2015**, *4*, 27066, doi:10.3402/jev.v4.27066.
28. Colombo, M.; Raposo, G.; Thery, C. Biogenesis, secretion, and intercellular interactions of exosomes and other

extracellular vesicles. *Annu Rev Cell Dev Biol* **2014**, *30*, 255-289, doi:10.1146/annurev-cellbio-101512-122326.

29. Witwer, K.W.; Buzas, E.I.; Bemis, L.T.; Bora, A.; Lasser, C.; Lotvall, J.; Nolte-'t Hoen, E.N.; Piper, M.G.; Sivaraman, S.; Skog, J., et al. Standardization of sample collection, isolation and analysis methods in extracellular vesicle research. *J Extracell Vesicles* **2013**, *2*, doi:10.3402/jev.v2i0.20360.
30. Fujita, Y.; Yoshioka, Y.; Ochiya, T. Extracellular vesicle transfer of cancer pathogenic components. *Cancer Sci* **2016**, *107*, 385-390, doi:10.1111/cas.12896.
31. Lawson, C.; Vicencio, J.M.; Yellon, D.M.; Davidson, S.M. Microvesicles and exosomes: new players in metabolic and cardiovascular disease. *J Endocrinol* **2016**, *228*, R57-71, doi:10.1530/joe-15-0201.
32. Andreola, G.; Rivoltini, L.; Castelli, C.; Huber, V.; Perego, P.; Deho, P.; Squarcina, P.; Accornero, P.; Lozupone, F.; Lugini, L., et al. Induction of lymphocyte apoptosis by tumor cell secretion of FasL-bearing microvesicles. *J Exp Med* **2002**, *195*, 1303-1316, doi:10.1084/jem.20011624.
33. Choi, D.; Spinelli, C.; Montermini, L.; Rak, J. Oncogenic Regulation of Extracellular Vesicle Proteome and Heterogeneity. *Proteomics* **2019**, *19*, e1800169, doi:10.1002/pmic.201800169.
34. Al-Nedawi, K.; Meehan, B.; Micallef, J.; Lhotak, V.; May, L.; Guha, A.; Rak, J. Intercellular transfer of the oncogenic receptor EGFRvIII by microvesicles derived from tumour cells. *Nat Cell Biol* **2008**, *10*, 619-624, doi:10.1038/ncb1725.
35. Vagner, T.; Spinelli, C.; Minciacchi, V.R.; Balaj, L.; Zandian, M.; Conley, A.; Zijlstra, A.; Freeman, M.R.; Demichelis, F.; De, S., et al. Large extracellular vesicles carry most of the tumour DNA circulating in prostate cancer patient plasma. *J Extracell Vesicles* **2018**, *7*, 1505403, doi:10.1080/20013078.2018.1505403.
36. Di Vizio, D.; Morello, M.; Dudley, A.C.; Schow, P.W.; Adam, R.M.; Morley, S.; Mulholland, D.; Rotinen, M.; Hager, M.H.; Insabato, L., et al. Large oncosomes in human prostate cancer tissues and in the circulation of mice with metastatic disease. *Am J Pathol* **2012**, *181*, 1573-1584, doi:10.1016/j.ajpath.2012.07.030.
37. Mebarek, S.; Abousalham, A.; Magne, D.; Do le, D.; Bandorowicz-Pikula, J.; Pikula, S.; Buchet, R. Phospholipases of mineralization competent cells and matrix vesicles: roles in physiological and pathological mineralizations. *Int J Mol Sci* **2013**, *14*, 5036-5129, doi:10.3390/ijms14035036.
38. Huang, Y.; Zucker, B.; Zhang, S.; Elias, S.; Zhu, Y.; Chen, H.; Ding, T.; Li, Y.; Sun, Y.; Lou, J., et al. Migrasome formation is mediated by assembly of micron-scale tetraspanin macrodomains. *Nat Cell Biol* **2019**, *21*, 991-1002, doi:10.1038/s41556-019-0367-5.
39. Kim, O.Y.; Park, H.T.; Dinh, N.T.H.; Choi, S.J.; Lee, J.; Kim, J.H.; Lee, S.W.; Gho, Y.S. Bacterial outer membrane vesicles suppress tumor by interferon-gamma-mediated antitumor response. *Nat Commun* **2017**, *8*, 626, doi:10.1038/s41467-017-00729-8.
40. Durcin, M.; Fleury, A.; Taillebois, E.; Hilairet, G.; Krupova, Z.; Henry, C.; Truchet, S.; Trotzmuller, M.; Kofeler, H.; Mabilleau, G., et al. Characterisation of adipocyte-derived extracellular vesicle subtypes identifies distinct protein and lipid signatures for large and small extracellular vesicles. *J Extracell Vesicles* **2017**, *6*, 1305677, doi:10.1080/20013078.2017.1305677.
41. Lee, T.H.; D'Asti, E.; Magnus, N.; Al-Nedawi, K.; Meehan, B.; Rak, J. Microvesicles as mediators of intercellular communication in cancer--the emerging science of cellular 'debris'. *Semin Immunopathol* **2011**, *33*, 455-467, doi:10.1007/s00281-011-0250-3.

42. Zhao, X.; Wu, X.; Qian, M.; Song, Y.; Wu, D.; Zhang, W. Knockdown of TGF-beta1 expression in human umbilical cord mesenchymal stem cells reverts their exosome-mediated EMT promoting effect on lung cancer cells. *Cancer Lett* **2018**, *428*, 34-44, doi:10.1016/j.canlet.2018.04.026.

43. Blackwell, R.H.; Foreman, K.E.; Gupta, G.N. The Role of Cancer-Derived Exosomes in Tumorigenicity & Epithelial-to-Mesenchymal Transition. *Cancers (Basel)* **2017**, *9*, doi:10.3390/cancers9080105.

44. Franzen, C.A.; Blackwell, R.H.; Todorovic, V.; Greco, K.A.; Foreman, K.E.; Flanigan, R.C.; Kuo, P.C.; Gupta, G.N. Urothelial cells undergo epithelial-to-mesenchymal transition after exposure to muscle invasive bladder cancer exosomes. *Oncogenesis* **2015**, *4*, e163, doi:10.1038/oncsis.2015.21.

45. Fujiwara, T.; Eguchi, T.; Sogawa, C.; Ono, K.; Murakami, J.; Ibaragi, S.; Asaumi, J.-i.; Calderwood, S.K.; Okamoto, K.; Kozaki, K.-i. Carcinogenic epithelial-mesenchymal transition initiated by oral cancer exosomes is inhibited by anti-EGFR antibody cetuximab. *Oral Oncology* **2018**, *86*, 251-257, doi:10.1016/j.oraloncology.2018.09.030.

46. Tauro, B.J.; Mathias, R.A.; Greening, D.W.; Gopal, S.K.; Ji, H.; Kapp, E.A.; Coleman, B.M.; Hill, A.F.; Kusebauch, U.; Hallows, J.L., et al. Oncogenic H-ras reprograms Madin-Darby canine kidney (MDCK) cell-derived exosomal proteins following epithelial-mesenchymal transition. *Mol Cell Proteomics* **2013**, *12*, 2148-2159, doi:10.1074/mcp.M112.027086.

47. Calderwood, S.K.; Gong, J. Heat Shock Proteins Promote Cancer: It's a Protection Racket. *Trends Biochem Sci* **2016**, *41*, 311-323, doi:10.1016/j.tibs.2016.01.003.

48. Ernst, A.; Anders, H.; Kapfhammer, H.; Orth, M.; Hennel, R.; Seidl, K.; Winssinger, N.; Belka, C.; Unkel, S.; Lauber, K. HSP90 inhibition as a means of radiosensitizing resistant, aggressive soft tissue sarcomas. *Cancer Lett* **2015**, *365*, 211-222, doi:10.1016/j.canlet.2015.05.024.

49. Wang, X.; Chen, M.; Zhou, J.; Zhang, X. HSP27, 70 and 90, anti-apoptotic proteins, in clinical cancer therapy (Review). *International journal of oncology* **2014**, *45*, 18-30, doi:10.3892/ijo.2014.2399.

50. Tang, D.; Khaleque, M.A.; Jones, E.L.; Theriault, J.R.; Li, C.; Wong, W.H.; Stevenson, M.A.; Calderwood, S.K. Expression of heat shock proteins and heat shock protein messenger ribonucleic acid in human prostate carcinoma in vitro and in tumors in vivo. *Cell Stress Chaperones* **2005**, *10*, 46-58.

51. Lonergan, P.E.; Tindall, D.J. Androgen receptor signaling in prostate cancer development and progression. *J Carcinog* **2011**, *10*, 20, doi:10.4103/1477-3163.83937.

52. Bang, Y.J.; Pirnia, F.; Fang, W.G.; Kang, W.K.; Sartor, O.; Whitesell, L.; Ha, M.J.; Tsokos, M.; Sheahan, M.D.; Nguyen, P., et al. Terminal neuroendocrine differentiation of human prostate carcinoma cells in response to increased intracellular cyclic AMP. *Proc Natl Acad Sci U S A* **1994**, *91*, 5330-5334.

53. Jongsma, J.; Oomen, M.H.; Noordzij, M.A.; Romijn, J.C.; van Der Kwast, T.H.; Schroder, F.H.; van Steenbrugge, G.J. Androgen-independent growth is induced by neuropeptides in human prostate cancer cell lines. *Prostate* **2000**, *42*, 34-44.

54. Klimstra, D.S.; Modlin, I.R.; Coppola, D.; Lloyd, R.V.; Suster, S. The pathologic classification of neuroendocrine tumors: a review of nomenclature, grading, and staging systems. *Pancreas* **2010**, *39*, 707-712, doi:10.1097/MPA.0b013e3181ec124e.

55. Kong, D.; Banerjee, S.; Ahmad, A.; Li, Y.; Wang, Z.; Sethi, S.; Sarkar, F.H. Epithelial to mesenchymal transition is mechanistically linked with stem cell signatures in prostate cancer cells. *PLoS One* **2010**, *5*, e12445,

doi:10.1371/journal.pone.0012445.

56. Zhang, Q.; Helfand, B.T.; Jang, T.L.; Zhu, L.J.; Chen, L.; Yang, X.J.; Kozlowski, J.; Smith, N.; Kundu, S.D.; Yang, G., et al. Nuclear factor-kappaB-mediated transforming growth factor-beta-induced expression of vimentin is an independent predictor of biochemical recurrence after radical prostatectomy. *Clin Cancer Res* **2009**, *15*, 3557-3567, doi:10.1158/1078-0432.ccr-08-1656.
57. Eguchi, T.; Prince, T.L.; Tran, M.T.; Sogawa, C.; Lang, B.J.; Calderwood, S.K. MZF1 and SCAND1 Reciprocally Regulate CDC37 Gene Expression in Prostate Cancer. *Cancers (Basel)* **2019**, *11*, doi:10.3390/cancers11060792.
58. Calderwood, S.K. Cdc37 as a co-chaperone to Hsp90. *Subcell Biochem* **2015**, *78*, 103-112, doi:10.1007/978-3-319-11731-7_5.
59. Gray, P.J., Jr.; Stevenson, M.A.; Calderwood, S.K. Targeting Cdc37 inhibits multiple signaling pathways and induces growth arrest in prostate cancer cells. *Cancer Res* **2007**, *67*, 11942-11950, doi:10.1158/0008-5472.CAN-07-3162.
60. Kimura, Y.; Rutherford, S.L.; Miyata, Y.; I., Y.; Freeman, B.C.; Yue, L.; Morimoto, R.I.; Lindquist, S. Cdc37 is a molecular chaperone with specific functions in signal transduction. *Genes & Development* **1997**, *11*, 1775-1785.
61. Silverstein, A.M.; Grammatikakis, N.; Cochran, B.H.; Chinkers, M.; Pratt, W.B. p50 cdc37 binds directly to the catalytic domain of Raf as well as to a site on hsp90 that is topologically adjacent to the tetratricopeptide repeat binding site. *J Biol Chem* **1998**, *273*, 20090-20095.
62. Chen, G.Y.; Cao, P.; Goeddel, D.V. TNF-induced recruitment and activation of the IKK complex require Cdc37 and Hsp90. *Mol Cell* **2002**, *9*, 401-410.
63. Dai, K.; Kobayashi, R.; Beach, D. Physical interactionof mammalian CDC37 with CDK4. *J Biol Chem* **1996**, *271*, 22030-22034.
64. Stepanova, L.; Leng, X.; Parker, S.B.; Harper, J.W. Mammalian p50 Cdc37 is aprotein kinase-targeting subunit of Hsp90 that binds and stabilize Cdk4. *Genes & Development* **1996**, *10*, 1491-1502.
65. Roe, S.M.; Ali, M.M.U.; Meyer, P.; Vaughan, C.K.; Panaretou, B.; Piper, P.W.; Prodromou, C.; Pearl, L.H. The mechanism of Hsp90 regulation by the protein kinase-specific cochaperone p50 cdc37. *Cell* **2004**, *116*, 87-98.
66. Stepanova, L.; Yang, G.; DeMayo, F.; Wheeler, T.M.; Finegold, M.; Thompson, T.C.; Harper, J.W. Induction of human CDC37 in prostate cancer correlates with the ability of targeted CDC37 expression to promote prostatic hyperplasia. *Oncogene* **2000**, *19*, 2186-2193.
67. Smith, J.R.; de Billy, E.; Hobbs, S.; Powers, M.; Prodromou, C.; Pearl, L.; Clarke, P.A.; Workman, P. Restricting direct interaction of CDC37 with HSP90 does not compromise chaperoning of client proteins. *Oncogene* **2015**, *34*, 15-26, doi:10.1038/onc.2013.519.
68. Neckers, L.; Workman, P. Hsp90 molecular chaperone inhibitors: are we there yet? *Clin Cancer Res* **2012**, *18*, 64-76, doi:10.1158/1078-0432.CCR-11-1000.
69. Tai, S.; Sun, Y.; Squires, J.M.; Zhang, H.; Oh, W.K.; Liang, C.Z.; Huang, J. PC3 is a cell line characteristic of prostatic small cell carcinoma. *Prostate* **2011**, *71*, 1668-1679, doi:10.1002/pros.21383.
70. Ware, J.L.; Paulson, D.F.; Mickey, G.H.; Webb, K.S. Spontaneous metastasis of cells of the human prostate carcinoma cell line PC-3 in athymic nude mice. *J Urol* **1982**, *128*, 1064-1067.
71. Eguchi, T.; Calderwood, S.K.; Takigawa, M.; Kubota, S.; Kozaki, K.I. Intracellular MMP3 Promotes HSP Gene Expression in Collaboration With Chromobox Proteins. *J Cell Biochem* **2017**, *118*, 43-51, doi:10.1002/jcb.25607.

72. Eguchi, T.; Kubota, S.; Kawata, K.; Mukudai, Y.; Uehara, J.; Ohgawara, T.; Ibaragi, S.; Sasaki, A.; Kuboki, T.; Takigawa, M. Novel transcription-factor-like function of human matrix metalloproteinase 3 regulating the CTGF/CCN2 gene. *Mol Cell Biol* **2008**, *28*, 2391-2413, doi:10.1128/MCB.01288-07.

73. Dreos, R.; Ambrosini, G.; Groux, R.; Cavin Perier, R.; Bucher, P. The eukaryotic promoter database in its 30th year: focus on non-vertebrate organisms. *Nucleic Acids Res* **2017**, *45*, D51-d55, doi:10.1093/nar/gkw1069.

74. Messeguer, X.; Escudero, R.; Farre, D.; Nunez, O.; Martinez, J.; Alba, M.M. PROMO: detection of known transcription regulatory elements using species-tailored searches. *Bioinformatics* **2002**, *18*, 333-334.

75. Eguchi, T.; Kubota, S.; Takigawa, M. Promoter Analyses of CCN Genes. *Methods Mol Biol* **2017**, *1489*, 177-185, doi:10.1007/978-1-4939-6430-7_18.

76. Namba, Y.; Sogawa, C.; Okusha, Y.; Kawai, H.; Itagaki, M.; Ono, K.; Murakami, J.; Aoyama, E.; Ohyama, K.; Asaumi, J.I., et al. Depletion of Lipid Efflux Pump ABCG1 Triggers the Intracellular Accumulation of Extracellular Vesicles and Reduces Aggregation and Tumorigenesis of Metastatic Cancer Cells. *Front Oncol* **2018**, *8*, 376, doi:10.3389/fonc.2018.00376.

77. Sogawa, C.; Eguchi, T.; Okusha, Y.; Ono, K.; Ohyama, K.; Iizuka, M.; Kawasaki, R.; Hamada, Y.; Takigawa, M.; Sogawa, N., et al. A reporter system evaluates tumorigenesis, metastasis, beta-catenin/MMP regulation, and druggability. *Tissue Eng Part A* **2019**, *25*, 1413-1425, doi:10.1089/ten.TEA.2018.0348.

78. Cirri, P.; Chiarugi, P. Cancer associated fibroblasts: the dark side of the coin. *Am J Cancer Res* **2011**, *1*, 482-497.

79. Gascard, P.; Tlsty, T.D. Carcinoma-associated fibroblasts: orchestrating the composition of malignancy. *Genes & Development* **2016**, *30*, 1002-1019, doi:10.1101/gad.279737.

80. Lu, H.; Clauser, K.R.; Tam, W.L.; Frose, J.; Ye, X.; Eaton, E.N.; Reinhardt, F.; Donnenberg, V.S.; Bhargava, R.; Carr, S.A., et al. A breast cancer stem cell niche supported by juxtacrine signalling from monocytes and macrophages. *Nat Cell Biol* **2014**, *16*, 1105-1117, doi:10.1038/ncb3041.

81. Calderwood, S.K. Heat shock proteins and cancer: intracellular chaperones or extracellular signalling ligands? *Philos Trans R Soc Lond B Biol Sci* **2018**, *373*, doi:10.1098/rstb.2016.0524.

82. Trepel, J.; Mollapour, M.; Giaccone, G.; Neckers, L. Targeting the dynamic HSP90 complex in cancer. *Nat Rev Cancer* **2010**, *10*, 537-549, doi:10.1038/nrc2887.

83. Fang, D.; Chen, H.; Zhu, J.Y.; Wang, W.; Teng, Y.; Ding, H.F.; Jing, Q.; Su, S.B.; Huang, S. Epithelial-mesenchymal transition of ovarian cancer cells is sustained by Rac1 through simultaneous activation of MEK1/2 and Src signaling pathways. *Oncogene* **2017**, *36*, 1546-1558, doi:10.1038/onc.2016.323.

84. Ke, L.; Xiang, Y.; Guo, X.; Lu, J.; Xia, W.; Yu, Y.; Peng, Y.; Wang, L.; Wang, G.; Ye, Y., et al. c-Src activation promotes nasopharyngeal carcinoma metastasis by inducing the epithelial-mesenchymal transition via PI3K/Akt signaling pathway: a new and promising target for NPC. *Oncotarget* **2016**, *7*, 28340-28355, doi:10.18632/oncotarget.8634.

85. Nagai, T.; Arao, T.; Furuta, K.; Sakai, K.; Kudo, K.; Kaneda, H.; Tamura, D.; Aomatsu, K.; Kimura, H.; Fujita, Y., et al. Sorafenib inhibits the hepatocyte growth factor-mediated epithelial mesenchymal transition in hepatocellular carcinoma. *Mol Cancer Ther* **2011**, *10*, 169-177, doi:10.1158/1535-7163.MCT-10-0544.

86. Larue, L.; Bellacosa, A. Epithelial-mesenchymal transition in development and cancer: role of phosphatidylinositol 3' kinase/AKT pathways. *Oncogene* **2005**, *24*, 7443-7454, doi:10.1038/sj.onc.1209091.

87. Hikita, T.; Kuwahara, A.; Watanabe, R.; Miyata, M.; Oneyama, C. Src in endosomal membranes promotes exosome secretion and tumor progression. *Sci Rep* **2019**, *9*, 3265, doi:10.1038/s41598-019-39882-z.

88. Corrado, C.; Saieva, L.; Raimondo, S.; Santoro, A.; De Leo, G.; Alessandro, R. Chronic myelogenous leukaemia exosomes modulate bone marrow microenvironment through activation of epidermal growth factor receptor. *J Cell Mol Med* **2016**, *20*, 1829-1839, doi:10.1111/jcmm.12873.

89. Zhang, H.; Deng, T.; Liu, R.; Bai, M.; Zhou, L.; Wang, X.; Li, S.; Wang, X.; Yang, H.; Li, J., et al. Exosome-delivered EGFR regulates liver microenvironment to promote gastric cancer liver metastasis. *Nat Commun* **2017**, *8*, 15016, doi:10.1038/ncomms15016.

90. Taverna, S.; Pucci, M.; Giallombardo, M.; Di Bella, M.A.; Santarpia, M.; Reclusa, P.; Gil-Bazo, I.; Rolfo, C.; Alessandro, R. Amphiregulin contained in NSCLC-exosomes induces osteoclast differentiation through the activation of EGFR pathway. *Sci Rep* **2017**, *7*, 3170, doi:10.1038/s41598-017-03460-y.

91. Kharmate, G.; Hosseini-Beheshti, E.; Caradec, J.; Chin, M.Y.; Tomlinson Guns, E.S. Epidermal Growth Factor Receptor in Prostate Cancer Derived Exosomes. *PLoS One* **2016**, *11*, e0154967, doi:10.1371/journal.pone.0154967.

92. Woodley, D.T.; Fan, J.; Cheng, C.F.; Li, Y.; Chen, M.; Bu, G.; Li, W. Participation of the lipoprotein receptor LRP1 in hypoxia-HSP90alpha autocrine signaling to promote keratinocyte migration. *J Cell Sci* **2009**, *122*, 1495-1498, doi:10.1242/jcs.047894.

93. Crow, J.; Atay, S.; Banskota, S.; Artale, B.; Schmitt, S.; Godwin, A.K. Exosomes as mediators of platinum resistance in ovarian cancer. *Oncotarget* **2017**, *8*, 11917-11936, doi:10.18632/oncotarget.14440.

94. Eguchi, T.; Ono, K.; Calderwood, S.K.; Okamoto, K. Exosome Release of Drugs: Coupling with Epithelial-Mesenchymal Transition. *Preprints* **2019**, doi:10.20944/preprints201912.0386.v1.

95. Tisza, M.J.; Zhao, W.; Fuentes, J.S.; Prijic, S.; Chen, X.; Levental, I.; Chang, J.T. Motility and stem cell properties induced by the epithelial-mesenchymal transition require destabilization of lipid rafts. *Oncotarget* **2016**, *7*, 51553-51568, doi:10.18632/oncotarget.9928.

96. Lauwers, E.; Wang, Y.C.; Gallardo, R.; Van der Kant, R.; Michiels, E.; Swerts, J.; Baatsen, P.; Zaiter, S.S.; McAlpine, S.R.; Gounko, N.V., et al. Hsp90 Mediates Membrane Deformation and Exosome Release. *Mol Cell* **2018**, *71*, 689-702.e689, doi:10.1016/j.molcel.2018.07.016.

97. Okusha, Y.; Eguchi, T.; Sogawa, C.; Okui, T.; Nakano, K.; Okamoto, K.; Kozaki, K.I. The intranuclear PEX domain of MMP involves proliferation, migration, and metastasis of aggressive adenocarcinoma cells. *J Cell Biochem* **2018**, *119*, 7363-7376, doi:10.1002/jcb.27040.

98. Wang, Y.; Theriault, J.R.; He, H.; Gong, J.; Calderwood, S.K. Expression of a dominant negative heat shock factor-1 construct inhibits aneuploidy in prostate carcinoma cells. *J Biol Chem* **2004**, *279*, 32651-32659, doi:10.1074/jbc.M401475200.